



Searches for a heavy scalar boson H decaying to a pair of 125 GeV Higgs bosons hh or for a heavy pseudoscalar boson A decaying to Zh , in the final states with $h \rightarrow \tau\tau$

The CMS Collaboration*

Abstract

A search for a heavy scalar boson H decaying into a pair of lighter standard-model-like 125 GeV Higgs bosons h and a search for a heavy pseudoscalar boson A decaying into a Z and an h boson are presented. The searches are performed on a dataset corresponding to an integrated luminosity of 19.7 fb^{-1} of pp collision data at a centre-of-mass energy of 8 TeV, collected by CMS in 2012. A final state consisting of two τ leptons and two b jets is used to search for the $H \rightarrow hh$ decay. A final state consisting of two τ leptons from the h boson decay, and two additional leptons from the Z boson decay, is used to search for the decay $A \rightarrow Zh$. The results are interpreted in the context of two-Higgs-doublet models. No excess is found above the standard model expectation and upper limits are set on the heavy boson production cross sections in the mass ranges $260 < m_H < 350 \text{ GeV}$ and $220 < m_A < 350 \text{ GeV}$.

Published in Physics Letters B as doi:10.1016/j.physletb.2016.01.056.

1 Introduction

The discovery of additional Higgs bosons at the LHC would provide direct evidence of physics beyond the standard model (SM). There are several types of models that require two Higgs doublets [1–3]. For example the minimal supersymmetric extension of the SM (MSSM) requires the introduction of an additional Higgs doublet, where one Higgs doublet couples to up-type quarks and the other to down-type quarks [4–11]. This leads to the prediction of five Higgs particles: one light and one heavy CP-even Higgs boson, h and H , one CP-odd Higgs boson A , and two charged Higgs bosons H^\pm [2, 12]. The masses and couplings of these bosons are interrelated and, at tree level, can be described by two parameters, which are often chosen to be the mass of the pseudoscalar boson m_A and the ratio of the vacuum expectation values of the neutral components of the two Higgs doublets $\tan\beta$. However, radiative corrections [13–17] introduce dependencies on other parameters namely the mass of the top quark m_t , the scale of the soft supersymmetry breaking masses M_{SUSY} , the higgsino mass parameter μ , the wino mass parameter M_2 , the third-generation trilinear couplings, A_t , A_b , and A_τ , the mass of the gluino $m_{\tilde{g}}$, and the third-generation slepton mass parameter $M_{\tilde{\ell}_3}$.

Direct searches for the neutral MSSM Higgs bosons have been performed by the CMS and ATLAS Collaborations [18–20] using the benchmark scenarios proposed in Ref. [21]. In these scenarios the parameters involved in the radiative corrections for the Higgs boson masses and couplings have been fixed, and only the two parameters m_A and $\tan\beta$ remain free. The value of M_{SUSY} was fixed at around 1 TeV, which produces a lightest CP-even Higgs boson with a mass m_h lower than the observed Higgs boson mass of 125.09 ± 0.21 (stat) ± 0.11 (syst) GeV [22], for values of $\tan\beta \lesssim 6$.

If, however, M_{SUSY} is much larger than 1 TeV, as suggested by the non-observations of SUSY partner particles at the LHC so far, low values of $\tan\beta$ can produce an h boson with $m_h \simeq 125$ GeV [23, 24]. The interpretation of the Higgs boson measurements in the framework of the recently developed MSSM benchmark scenarios [24–27] suggests that the mass of the CP-odd Higgs boson, m_A , can be smaller than $2m_t$. In the mass region below $2m_t$ and at low values of $\tan\beta$, the decay mode of the heavy scalar $H \rightarrow hh$ and that of the pseudoscalar $A \rightarrow Zh$ can have sizeable branching fractions.

This encourages a programme of searches in the so-called “low $\tan\beta$ ” channels [23, 28]:

- for $220 \text{ GeV} < m_A < 2m_t$: $A \rightarrow Zh$;
- for $260 \text{ GeV} < m_A < 2m_t$: $H \rightarrow hh$;
- for $m_A > 2m_t$: $A/H \rightarrow t\bar{t}$.

The decay modes $H \rightarrow hh$ and $A \rightarrow Zh$, studied in this paper, are also present in other types of two-Higgs-doublet models (2HDM) [2, 3]. There are different types of 2HDM with those most similar to the MSSM (i.e. where up-type fermions couple to one doublet and down-type fermions to the other) being “Type II” 2HDM. The discovery of a Higgs boson at the LHC [29–31] with a mass around 125 GeV pushes the 2HDM parameter space towards either the alignment or decoupling limits [24]. In these limits the properties of h are SM-like.

In the alignment limit of 2HDM when $\cos(\beta - \alpha) \ll 1$ (where α is the mixing angle between the two neutral scalar fields), the Hhh and AZh couplings vanish at Born level [32]. However, in the MSSM, the Hhh and AZh couplings do not vanish, even in the alignment limit, because of the large radiative corrections that arise in the model. In the decoupling limit of 2HDM the scalar Higgs boson H has a very large mass and the decay $H \rightarrow t\bar{t}$ dominates [32].

This paper reports the results of searches for the decays $H \rightarrow hh \rightarrow bb\tau\tau$ and $A \rightarrow Zh \rightarrow \ell\ell\tau\tau$

(where $\ell\ell$ denotes $\mu\mu$ or ee). The choice of τ pair final state was driven by its quite clean signature and by the most recent results, which gave stronger evidence of the 125 Higgs boson coupling to the fermions [33]. This analysis exploits similar techniques as used for the search for the SM Higgs boson at 125 GeV [34] and several different $\tau\tau$ signatures are studied. For the channel $H \rightarrow hh \rightarrow bb\tau\tau$, the $\mu\tau_h$, $e\tau_h$, and $\tau_h\tau_h$ final states are used, where τ_h denotes the visible products of a hadronically decaying τ , whereas for the channel $A \rightarrow Zh \rightarrow \ell\ell\tau\tau$, the $\mu\tau_h$, $e\tau_h$, $\tau_h\tau_h$, and $e\mu$ final states are selected.

Searches for the decays $H \rightarrow hh$, and $A \rightarrow Zh$ have already been performed by the ATLAS [35–38] and CMS Collaborations [39–41] in di-photon, multilepton and bb final states.

This analysis has the power to bring important results in the low $\tan\beta$ region for the m_A range, which has been previously discussed and where these processes have an enhanced sensitivity [23]. This region has not yet been excluded by the direct or indirect searches for a heavy scalar or pseudoscalar Higgs boson, that have been mentioned above, therefore the described decay modes look to be quite promising.

For simplicity of the paper, we are neither indicating the charge of the leptons nor the particle-antiparticle nature of quarks.

2 The CMS detector, simulation and data samples

A detailed description of the CMS detector can be found in Ref. [42]. The central feature of the CMS apparatus is a superconducting solenoid of 6 m internal diameter providing a field of 3.8 T. Within the field volume are a silicon pixel and strip tracker, a crystal electromagnetic calorimeter (ECAL), and a brass/scintillator hadron calorimeter. Muons are measured in gas-ionisation detectors embedded in the steel return yoke of the magnet.

The CMS coordinate system has the origin centered at the nominal collision point and is oriented such that the x -axis points to the center of the LHC ring, the y -axis points vertically upward and the z -axis is in the direction of the beam. The azimuthal angle ϕ is measured from the x -axis in the xy plane and the radial coordinate in this plane is denoted by r . The polar angle θ is defined in the rz plane and the pseudorapidity is $\eta = -\ln[\tan(\theta/2)]$ [42]. The momentum component transverse to the beam direction, denoted by p_T , is computed from the x - and y -components.

The first level (L1) of the CMS trigger system, composed of custom hardware processors, uses information from the calorimeters and muon detectors to select the most interesting events in a fixed time interval of less than 4 μ s. The high-level Trigger processor farm decreases the L1 accept rate from around 100 kHz to less than 1 kHz before data storage.

The data used for this search were recorded with the CMS detector in proton-proton collisions at the CERN LHC and correspond to an integrated luminosity of 19.7 fb^{-1} at a centre-of-mass energy of $\sqrt{s} = 8$ TeV. The $H \rightarrow hh$ signals are modelled with the PYTHIA 6.4.26 [43] event generator while the $A \rightarrow Zh$ signals were modelled with MADGRAPH 5.1 [44]. When modelling background processes, the MADGRAPH 5.1 generator is used for Z +jets, W +jets, $t\bar{t}$, and diboson production, and POWHEG 1.0 [45–48] for single top quark production. The POWHEG and MADGRAPH generators are interfaced with PYTHIA for parton showering and fragmentation using the Z2* tune [49]. All generators are interfaced with TAUOLA [50] for the simulation of the τ decays. All generated events are processed through a detailed simulation of the CMS detector based on GEANT4 [51] and are reconstructed with the same algorithms as the data. Parton distribution functions (PDFs) CT10 [52] or CTEQ6L1 [53] for the proton are used, de-

pending on the generator in question, together with MSTW2008 [54] according to PDF4LHC prescriptions [55].

3 Event reconstruction

During the 2012 LHC run there were an average of 21 proton-proton interactions per bunch crossing. The collision vertex that maximizes the sum of the squares of momenta components perpendicular to the beamline (transverse momenta) of all tracks associated with it, $\sum p_T^2$, is taken to be the vertex of the primary hard interaction. The other vertices are categorised as pileup vertices.

A particle-flow algorithm [56, 57] is used to reconstruct individual particles, i.e. muons, electrons, photons, charged hadrons and neutral hadrons, using information from all CMS subdetectors. Composite objects such as jets, hadronically decaying τ leptons, and missing transverse energy are then constructed using the lists of individual particles.

Muons are reconstructed by performing a simultaneous global track fit to hits in the silicon tracker and the muon system [58]. Electrons are reconstructed from clusters of ECAL energy deposits matched to hits in the silicon tracker [59]. Muons and electrons assumed to originate from W or Z boson decays are required to be spatially isolated from other particles [59, 60]. The presence of charged and neutral particles from pileup vertices is taken into account in the isolation requirement of both muons and electrons. Muon and electron identification and isolation efficiencies are measured via the tag-and-probe technique [61] using inclusive samples of $Z \rightarrow \ell\ell$ events from data and simulation. Correction factors are applied to account for differences between data and simulation.

Jets are reconstructed from all particles using the anti- k_T jet clustering algorithm implemented in FASTJET [62, 63] with a distance parameter of 0.5. The contribution to the jet energy from particles originating from pileup vertices is removed following a procedure based on the effective jet area described in Ref. [64]. Furthermore, jet energy corrections are applied as a function of jet p_T and η correcting jet energies to the generator level response of the jet, on average. Jets originating from pileup interactions are removed by a multivariate pileup jet identification algorithm [65].

The missing transverse momentum vector \vec{p}_T^{miss} is defined as the negative vector sum of the transverse momenta of all reconstructed particles in the volume of the detector (electrons, muons, photons, and hadrons). Its magnitude is referred to as E_T^{miss} . The E_T^{miss} reconstruction is improved by taking into account the jet energy scale corrections and the ϕ modulation, due to collisions not being at the nominal centre of CMS [66]. A multivariate regression correction of E_T^{miss} , where the contributing particles are separated into those coming from the primary vertex and those that are not, mitigates the effect of pileup [66].

Jets from the hadronisation of b-quarks (b jets) are identified with the combined secondary vertex (CSV) b tagging algorithm [67], which exploits the information on the decay vertices of long-lived mesons and the transverse impact parameter measurements of charged particles. This information is combined in a likelihood discriminant. The medium value of the CSV discriminator, corresponding to a b jet misidentification probability of 1%, has been used in this analysis.

Hadronically decaying τ leptons are reconstructed using the hadron-plus-strips algorithm [68], which considers candidates with one charged pion and up to two neutral pions, or three charged pions. The neutral pions are reconstructed as “strips” of electromagnetic particles

taking into account possible broadening of calorimeter energy depositions in the ϕ direction from photon conversions. The τ_h candidates that are also compatible with muons or electrons are rejected. Jets originating from the hadronization of quarks and gluons are suppressed by requiring the τ_h candidate to be isolated. The contribution of charged and neutral particles from pileup interactions is removed when computing the isolation.

4 Event selection

The events are selected with a combination of electron, muon and τ trigger objects [34, 59, 60, 69]. The identification criteria of these objects were progressively tightened and their transverse momentum thresholds raised as the LHC instantaneous luminosity increased over the data taking period. A tag-and-probe method was used to measure the efficiencies of these triggers in data and simulation, and correction factors are applied to the simulation.

Electrons, muons, and τ_h are selected using the criteria defined in the CMS search for the SM Higgs boson at 125 GeV [34]. Specific requirements for the selection of the $H \rightarrow hh \rightarrow bb\tau\tau$ and the $A \rightarrow Zh \rightarrow \ell\ell\tau\tau$ channels are described below.

4.1 Event selection of $H \rightarrow hh \rightarrow bb\tau\tau$

In the $H \rightarrow hh \rightarrow bb\tau\tau$ channel, the three most sensitive final states are analysed, distinguished by the decay mode of the two τ leptons originating from the h boson ($\mu\tau_h$, $e\tau_h$ and $\tau_h\tau_h$).

In the $\mu\tau_h$ and $e\tau_h$ final states, events are selected with a muon with $p_T > 20$ GeV and $|\eta| < 2.1$ or an electron of $p_T > 24$ GeV and $|\eta| < 2.1$, and an oppositely charged τ_h of $p_T > 20$ GeV and $|\eta| < 2.3$. To reduce the $Z \rightarrow \mu\mu, ee$ contamination, events with two muons or electrons of $p_T > 15$ GeV, of opposite charges, and passing loose isolation criteria are rejected.

In the $\mu\tau_h$ and $e\tau_h$ final states, the transverse mass of the muon or electron and \vec{p}_T^{miss}

$$m_T = \sqrt{2p_T E_T^{\text{miss}}(1 - \cos \Delta\phi)}, \quad (1)$$

where p_T is the lepton transverse momentum and $\Delta\phi$ is the difference in the azimuthal angle between the lepton momentum and \vec{p}_T^{miss} , is required to be less than 30 GeV to reject events coming from W +jets and $t\bar{t}$ backgrounds. The m_T distribution for the $\mu\tau_h$ final state is shown in Fig. 1.

In the $\tau_h\tau_h$ final state, events with two oppositely charged hadronically decaying τ leptons with $p_T > 45$ GeV and $|\eta| < 2.1$ are selected.

In addition to the $\tau\tau$ selection, each selected event must contain at least two jets with $p_T > 20$ GeV and $|\eta| < 2.4$. These p_T and η requirements are necessary to select jets that have a well defined value of the CSV discriminator (Section 3), which is important for categorising signal-like events with two b jet candidates coming from the 125 GeV Higgs boson decaying to bb .

Simulation studies show that the majority of signal events will have at least one jet passing the medium working point of the CSV discriminator. The jets are ordered by CSV discriminator value, such that the leading and subleading jets are defined as those with the two highest CSV values. Then the events are separated into categories, defined as:

- 2jet-0tag when neither the leading nor subleading jets passes the medium CSV working point. Only a small amount of signal is collected in this category, which is background-dominated.

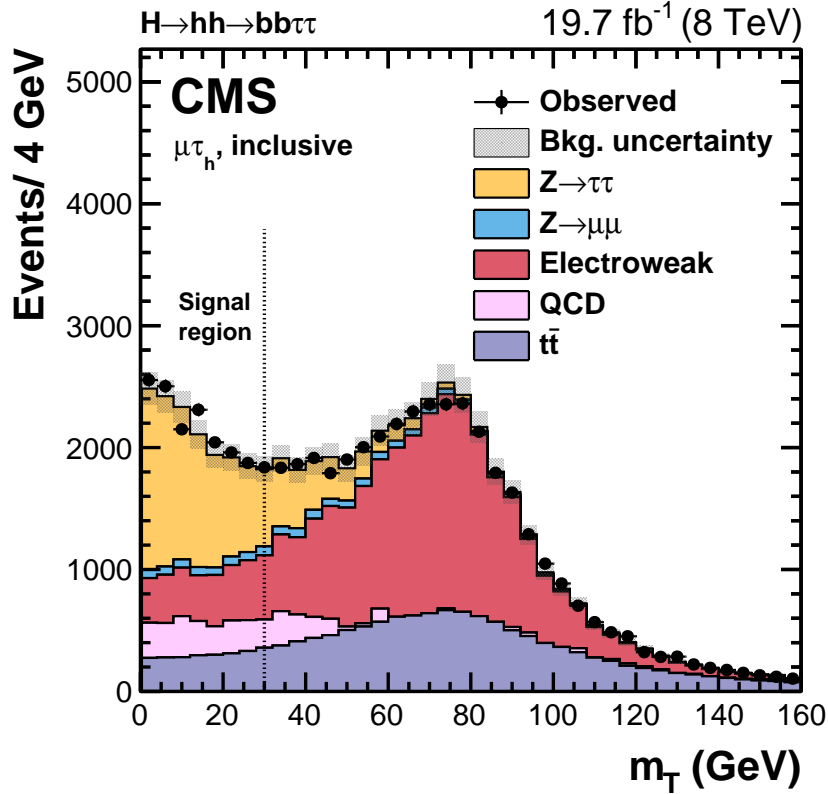


Figure 1: Distribution of m_T for events in the $\mu\tau_h$ final state, containing at least two additional jets. The W +jets background is included in the “electroweak” category. Multijet events are indicated as QCD. The $H \rightarrow hh \rightarrow bb\tau\tau$ selection requires $m_T < 30$ GeV for the $\mu\tau_h$ and $e\tau_h$ final states.

- 2jet–1tag when only the leading but not the subleading jet passes the medium CSV working point.
- 2jet–2tag when both the leading and subleading jets pass the medium CSV working point.

The signal extraction is performed using the distribution of the reconstructed mass of the H boson candidate.

4.2 Event selection of $A \rightarrow Zh \rightarrow \ell\ell\tau\tau$

In the $A \rightarrow Zh \rightarrow \ell\ell\tau\tau$ channel eight final states are analysed. These are categorised according to the decay mode of the Z boson and the decay mode of the τ leptons originating from the h boson.

The Z boson is reconstructed from two same-flavour, isolated, and oppositely charged electrons or muons. In the $Z \rightarrow \mu\mu$ (ee) final state the muons (electrons) are required to have $|\eta| < 2.4$ (2.5) with $p_T > 20$ GeV for the leading lepton and $p_T > 10$ GeV for the subleading lepton. The invariant mass of the two leptons is required to be between 60 GeV and 120 GeV. When more than one pair of leptons satisfy these criteria, the pair with an invariant mass closest to the Z boson mass is selected.

After the Z candidate has been chosen, the $h \rightarrow \tau\tau$ decay is selected by combining the decay products of the two τ leptons in the four final states $\mu\tau_h, e\tau_h, \tau_h\tau_h, e\mu$. The combination of the

large contribution from the irreducible ZZ background and of the small branching fractions of leptonic tau decays makes the $\mu\mu$ and ee final states less sensitive to the signal, and therefore they are not used in the analysis. Depending on the final state, a muon with $p_T > 10$ GeV and $|\eta| < 2.4$, or an electron of $p_T > 10$ GeV and $|\eta| < 2.5$, or a τ_h of $p_T > 21$ GeV and $|\eta| < 2.3$ are combined to form an oppositely charged pair. Events with additional light leptons satisfying these requirements are rejected.

A requirement on L_T^h , which is the scalar sum of the visible transverse momenta of the two τ candidates originating from the h boson, is applied to lower the reducible background from misidentified leptons as well as the irreducible background from ZZ production. The thresholds of this requirement depend on the final state and have been chosen in such a way as to optimise the sensitivity of the analysis to the presence of an $A \rightarrow Zh$ signal for A masses between 220 and 350 GeV. The distribution of L_T^h for events in the $\ell\ell\tau_h\tau_h$ final state can be seen in Fig. 2.

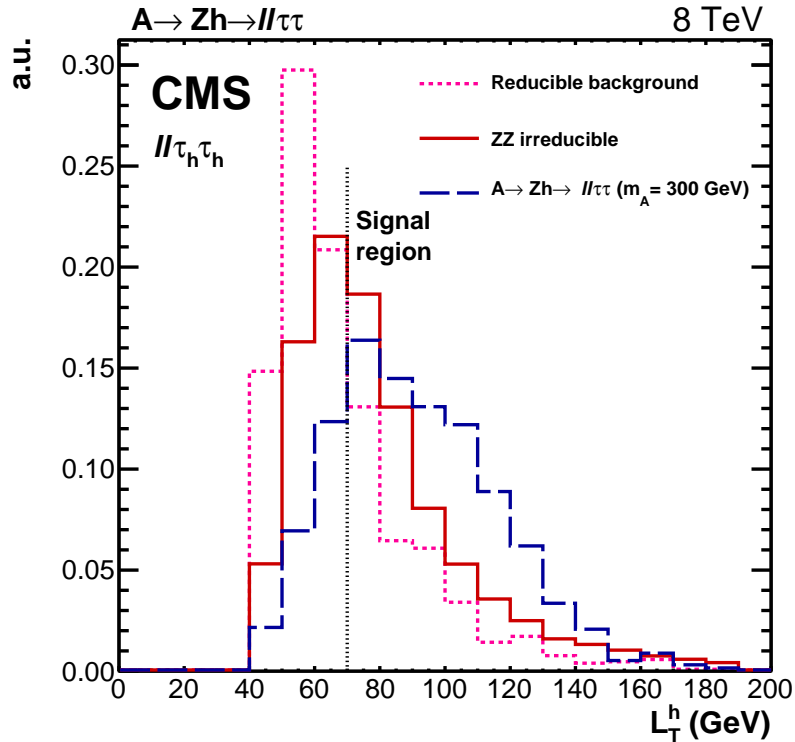


Figure 2: Distribution of the variable L_T^h for events in the $\ell\ell\tau_h\tau_h$ final state. The reducible background is estimated from data, instead the ZZ irreducible background from simulation.

In order to reduce the $t\bar{t}$ background, events containing a jet with $p_T > 20$ GeV, $|\eta| < 2.4$ and passing the medium working point of the CSV b tagging discriminator are removed.

The four final objects are further required to be separated from each other by $\Delta R = \sqrt{(\Delta\eta)^2 + (\Delta\phi)^2}$ larger than 0.5 (where phi is in radians), and to come from the same primary vertex.

In this channel the signal extraction is performed using the distribution of the reconstructed mass of the A boson candidate.

5 Background estimation

5.1 Background estimation for $H \rightarrow hh \rightarrow bb\tau\tau$

The backgrounds to the $H \rightarrow hh \rightarrow bb\tau\tau$ final state consist predominantly of $t\bar{t}$ events, followed by $Z \rightarrow \tau\tau$ +jets events, W +jets events, and QCD multijet events, with other small contributions from $Z \rightarrow \ell\ell$, diboson, and single top quark production. The estimation of the shapes of the reconstructed H mass and of the yields of the major backgrounds is obtained from data wherever possible.

The $Z \rightarrow \tau\tau$ process constitutes an irreducible background due to its final state involving two τ leptons, which only differ from the $h \rightarrow \tau\tau$ signal by having an invariant mass closer to the mass of the Z boson instead of the Higgs boson. Requiring two jets in the event greatly reduces this background and the b tagging requirements reduce it even further. Nevertheless, it still remains an important source of background events, in particular in the 2jet–1tag and 2jet–0tag categories. This background is estimated using a sample of $Z \rightarrow \mu\mu$ events from data, obtained by requiring two oppositely charged isolated muons, where the reconstructed muons are replaced by the reconstructed particles from simulated τ decays. A correction for a contamination from $t\bar{t}$ events is applied to the $Z \rightarrow \mu\mu$ selection. This technique substantially reduces the systematic uncertainties due to the jet energy scale and the missing transverse energy, as these quantities are modelled with data.

For the $t\bar{t}$ background, both shape and normalisation are taken from Monte Carlo simulation (MC), and the results are checked against data in a control region where the presence of $t\bar{t}$ events is enhanced by requiring $e\mu$ in the final state instead of a ditau, and at least one b tagged jet.

Another significant source of background is from QCD multijet events, which can mimic the signal in various ways, e.g. where one or more jets are misidentified as τ_h . In the $\mu\tau_h$ and $e\tau_h$ channels, the shape of the QCD background is estimated using an observed sample of same-sign (SS) $\tau\tau$ events. The yield is obtained by scaling the observed number of SS events by the ratio of the opposite-sign (OS) to SS event yields obtained in a QCD-enriched region with relaxed lepton isolation. In the $\tau_h\tau_h$ channel, the shape is obtained from OS events with relaxed τ isolation. The yield is obtained by scaling these events by the ratio of SS events with tighter and relaxed τ isolation.

In the $\mu\tau_h$ and $e\tau_h$ channels, W +jets events in which there is a jet misidentified as a τ_h are another sizeable source of background. The W +jets shape is modelled using MC simulation and the yield is estimated using a control region of events with large m_T close to the W mass. In the $\tau_h\tau_h$ channel this background has been found to be less relevant and its shape and yield are taken from MC simulation.

The contribution of Drell–Yan production of muon and electron pairs is estimated from simulation after rescaling the simulated yield to that measured from observed $Z \rightarrow \mu\mu$ events. In the $e\tau_h$ channel, the $Z \rightarrow ee$ simulation is further corrected using the $e \rightarrow \tau_h$ misidentification rate measured in data using a tag-and-probe technique [61] on $Z \rightarrow ee$ events.

Finally the contributions of other minor backgrounds such as diboson and single top quark events are estimated from simulation. Possible contributions from SM Higgs boson production are estimated and found to have a negligible effect on the final result.

5.2 Background estimation for $A \rightarrow Zh \rightarrow \ell\ell\tau\tau$

The backgrounds to the $A \rightarrow Zh$ channel can be divided into a reducible component and an irreducible component which contribute in equal parts.

The predominant source of irreducible background is from ZZ production that yields exactly the same final states as the expected signal. Other “rare” sources of irreducible background are SM Higgs boson associated production with a Z boson, $t\bar{t}Z$ production where the Z boson decays into a muon or an electron pair and both top quarks decay leptonically (to e, μ , or τ_h), and triboson events (WWZ, WZZ, ZZZ). The contributions of all the irreducible backgrounds after the final selection are estimated from simulation.

The reducible backgrounds have at least one lepton in the final state that is due to a misidentified jet that passes the lepton identification. In $\ell\ell\tau_h\tau_h$ final states, the reducible background is essentially composed of Z+jets events with at least two jets, whereas in $\ell\ell\mu\tau_h$ and $\ell\ell e\tau_h$ final states, the main contribution to the reducible background comes from WZ+jets with three light leptons. The contribution from these processes to the final selected events is estimated using control samples in data.

The probabilities for a jet that passes relaxed lepton selection criteria to pass the final identification and isolation criteria of electrons, muons, and τ leptons are measured in a signal-free region as a function of the transverse momentum of the object closest to the candidate, $f(p_T^{\text{fake}})$. In this region, events are required to pass all the final state selections, except that the reconstructed τ candidates are required to have the same sign and to pass relaxed identification and isolation criteria. This effectively eliminates any possible signal, while maintaining roughly the same proportion of reducible background events.

In order to use the misidentification probabilities $f(p_T^{\text{fake}})$, sidebands are defined for each channel, where, unlike the relaxed criterion, the final identification or isolation criterion is not satisfied for one or more of the final state lepton candidates. The number of reducible background events due to a lepton being misidentified in the final selection is estimated by applying the weight $f(p_T^{\text{fake}})/(1 - f(p_T^{\text{fake}}))$ to the observed events with lepton candidates in the sideband that satisfy the relaxed but not the final identification or isolation criterion. Finally, the reducible background shape of the reconstructed A mass is obtained from a SS signal-free region where the τ candidates have the same charge and relaxed isolation criteria. Possible contributions from SM Higgs boson production are estimated and found to have a negligible effect on the final result.

6 Systematic uncertainties

The shape of the reconstructed mass of the A and H boson candidates, used for signal extraction, and the normalisation are sensitive to various systematic uncertainties.

The main contributions to the normalisation uncertainty that affect the signal and the simulated backgrounds include the uncertainty in the total integrated luminosity, which amounts to 2.6% [70], and the identification and trigger efficiencies of muons (2%) and electrons (2%). The τ_h identification efficiency has a 6% uncertainty (8% in the $\tau_h\tau_h$ channel), which is measured in $Z/\gamma^* \rightarrow \tau\tau \rightarrow \mu\tau_h$ events using a tag-and-probe technique. There is a 3% uncertainty in the efficiency on the hadronic part of the $\mu\tau_h$ and $e\tau_h$ triggers, and a 4.5% uncertainty on each of the two τ_h candidates required by the $\tau_h\tau_h$ trigger. The b tagging efficiency has an uncertainty of 2–7%, and the mistag rate for light-flavour partons is accurate to 10–20% depending on η and p_T [67]. The background normalisation uncertainties from the estimation methods discussed

in Section 5 are also considered. In the $H \rightarrow hh \rightarrow bb\tau\tau$ channel this uncertainties amount to 2–40% depending on the event category and on the final state. The uncertainties of reducible backgrounds to the $A \rightarrow Zh$ channel are estimated by evaluating an individual uncertainty for each lepton misidentification rate and applying it to the background calculation. This amounts to 15–50% depending on the final $\ell\ell\tau\tau$ state considered. The main uncertainty in the estimation of the ZZ background arises from the theoretical uncertainty in the ZZ production cross section.

Uncertainties that contribute to variations in the shape of the mass spectrum include the jet energy scale, which varies with jet p_T and jet η [71], and the τ lepton (3%) energy scale [34].

Theoretical uncertainties on the cross section for signal derive from PDF and QCD scale uncertainties and depend on the choice of signal hypothesis. For model independent results no choice of cross section is made and hence no theoretical uncertainties are considered. For the MSSM interpretation the uncertainties depend on m_A and $\tan\beta$ and amount to 2–3% for PDF uncertainties and 5–9% for scale uncertainties, evaluated as described in [27] and using the PDF4LHC recommendations [55]. No theoretical uncertainties are considered in the 2HDM interpretation.

7 Results and interpretation

The ditau ($m_{\tau\tau}$) mass is reconstructed using a dedicated algorithm called SVFIT [72], which combines the visible four-vectors of the τ lepton candidates as well as the E_T^{miss} and its experimental resolution in a maximum likelihood estimator.

For the $H \rightarrow hh \rightarrow bb\tau\tau$ process, the chosen distribution for signal extraction is the four-body mass. The decay products of the two h bosons need to fulfill stringent kinematic constraints, due to the small natural width of the h . These constraints can be used in a kinematic fit in order to improve the event reconstruction and to better separate signal events from background. The collinear approximation for the decay products of the τ leptons is assumed in the fit, since the τ leptons are highly boosted as they originate from an object that is heavy when compared to their own mass. Furthermore, it is assumed that the reconstruction of the directions of all final state objects is accurate and the uncertainties can be neglected compared to the uncertainties on the energy reconstruction. In the decay of the two τ leptons, at least two neutrinos are involved and there is no precise measurement of the original τ lepton energies. For this reason, the τ lepton energies are constrained from the balance of the fitted H boson transverse momentum and the reconstructed transversal recoil determined from E_T^{miss} reconstruction algorithms, as described in Sec. 3. The reconstructed mass obtained with the kinematic fit is denoted by m_H^{kinfit} (see Appendix A for a detailed description).

The signal-to-background ratio is greatly improved by selecting events that are consistent with a mass of 125 GeV for both the dijet (m_{bb}) mass and the ditau mass ($m_{\tau\tau}$) reconstructed with SVFIT. The mass windows of the selections are optimised to collect as much signal as possible while rejecting a large part of the background. They correspond to $70 < m_{bb} < 150$ GeV and $90 < m_{\tau\tau} < 150$ GeV. The invariant mass distributions of the H boson in different final states are shown in Figs. 3, 4 and 5.

For the $A \rightarrow Zh \rightarrow \ell\ell\tau\tau$ process, the A boson mass is reconstructed from the four-vector information of the Z boson candidate and the four-vector information of the h boson candidate as obtained from SVFIT. The invariant mass distributions of the A boson in the different final states are shown in Figs. 6 and 7. The $\ell\ell\tau_h\tau_h$ final states have a comparable contribution

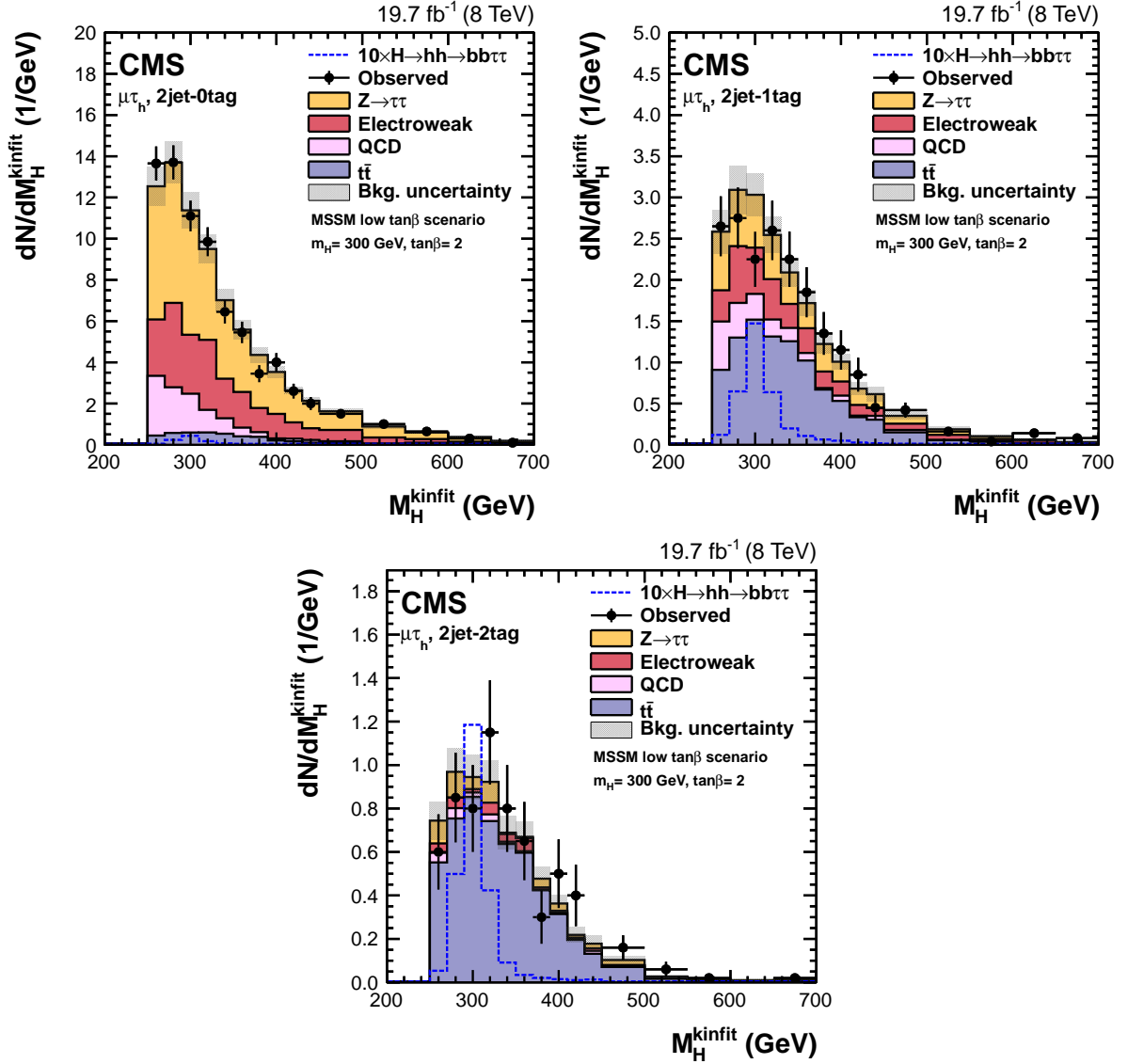


Figure 3: Distributions of the reconstructed four-body mass with the kinematic fit after applying mass selections on $m_{\tau\tau}$ and m_{bb} in the $\mu\tau_h$ channel. The plots are shown for events in the 2jet-0tag (top left), 2jet-1tag (top right), and 2jet-2tag (bottom) categories. The expected signal scaled by a factor 10 is shown superimposed as an open dashed histogram for $\tan\beta = 2$ and $m_H = 300$ GeV in the low $\tan\beta$ scenario of the MSSM. Expected background contributions are shown for the values of nuisance parameters (systematic uncertainties) obtained after fitting the signal plus background hypothesis to the data.

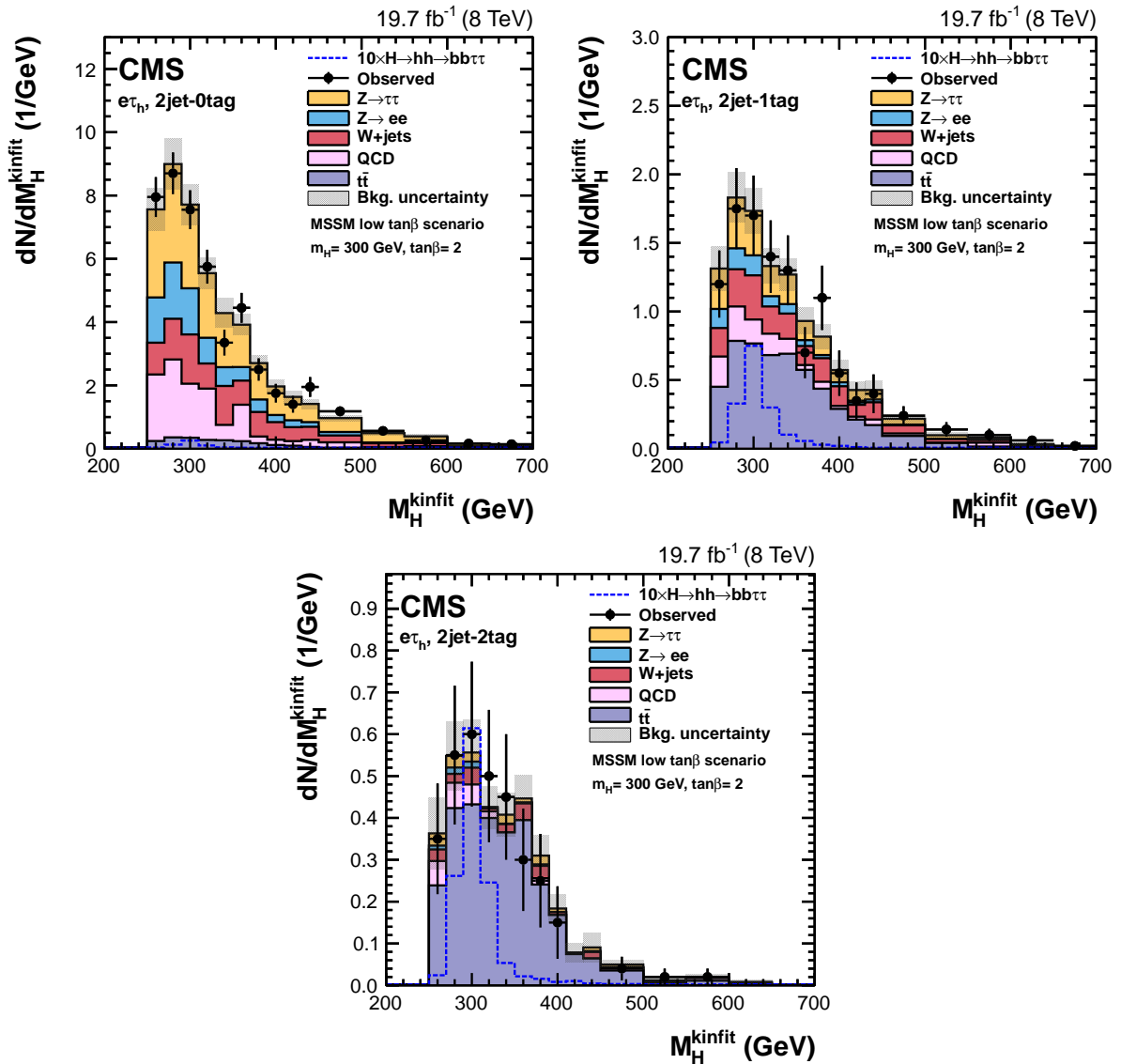


Figure 4: Distributions of the reconstructed four-body mass with the kinematic fit after applying mass selections on $m_{\tau\tau}$ and m_{bb} in the $e\tau_h$ channel. The plots are shown for events in the 2jet-0tag (top left), 2jet-1tag (top right), and 2jet-2tag (bottom) categories. The expected signal scaled by a factor 10 is shown superimposed as an open dashed histogram for $\tan\beta = 2$ and $m_H = 300 \text{ GeV}$ in the low $\tan\beta$ scenario of the MSSM. Expected background contributions are shown for the values of nuisance parameters (systematic uncertainties) obtained after fitting the signal plus background hypothesis to the data.

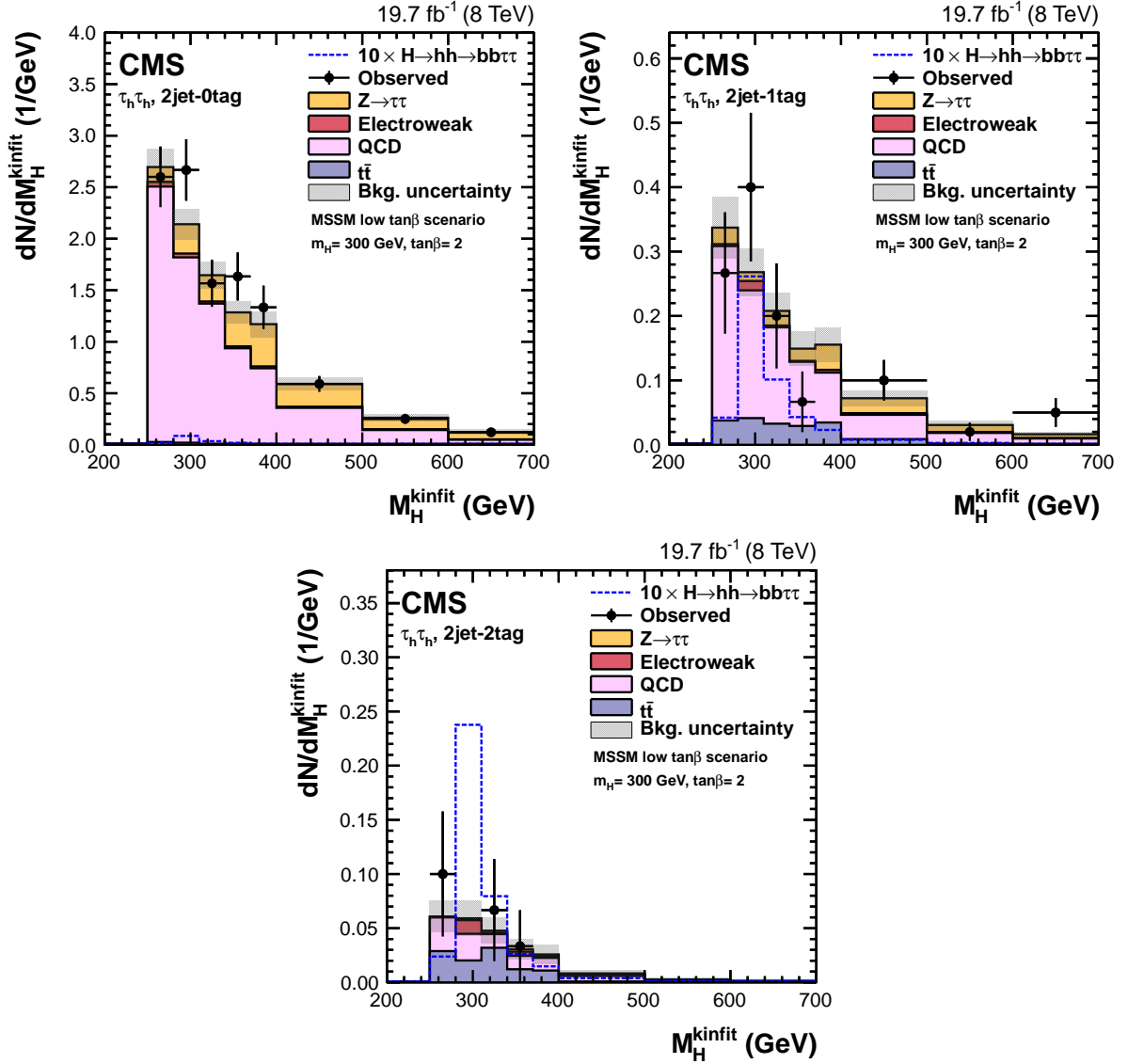


Figure 5: Distributions of the reconstructed four-body mass with the kinematic fit after applying mass selections on $m_{\tau\tau}$ and m_{bb} in the $\tau_h \tau_h$ channel. The plots are shown for events in the 2jet-0tag (top left), 2jet-1tag (top right), and 2jet-2tag (bottom) categories. The expected signal scaled by a factor 10 is shown superimposed as an open dashed histogram for $\tan\beta = 2$ and $m_H = 300$ GeV in the low $\tan\beta$ scenario of the MSSM. Expected background contributions are shown for the values of nuisance parameters (systematic uncertainties) obtained after fitting the signal plus background hypothesis to the data.

from reducible and irreducible backgrounds, while the $\ell\ell e\mu$ final states are dominated by the irreducible ZZ production. The background is labelled as “rare” collects together the smaller contributions from the triboson processes as discussed in the previous section.

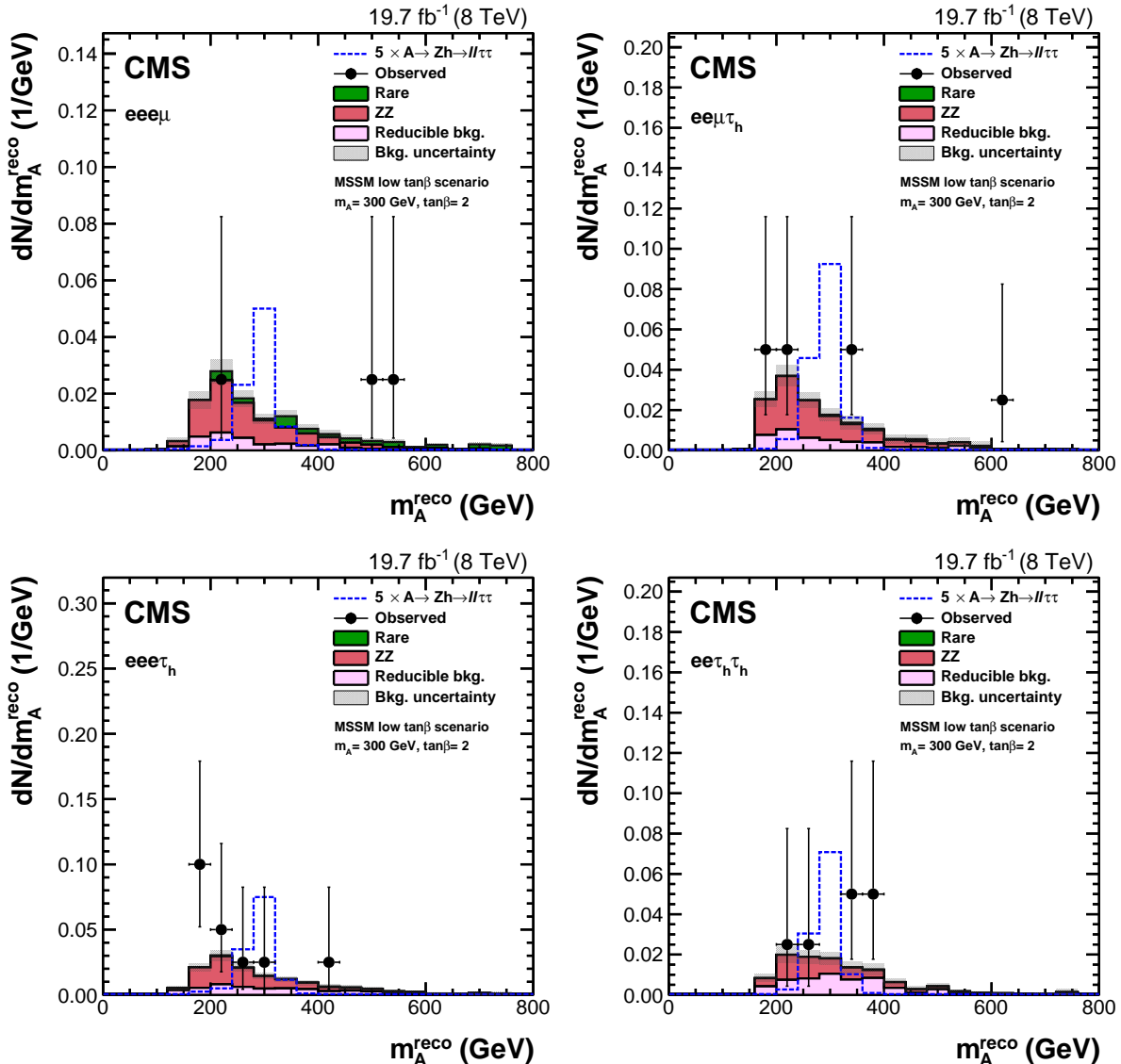


Figure 6: Invariant mass distributions for different final states of the $A \rightarrow Zh$ process where Z decays to ee . The expected signal scaled by a factor 5 is shown superimposed as an open dashed histogram for $\tan\beta = 2$ and $m_A = 300$ GeV in the low $\tan\beta$ scenario of MSSM. Expected background contributions are shown for the values of nuisance parameters (systematic uncertainties) obtained after fitting the signal plus background hypothesis to the data.

In neither search do the invariant mass spectra show any evidence of a signal. Model independent upper limits at 95% confidence level (CL) on the cross section times branching fraction are set using a binned maximum likelihood fit for the *signal plus background* and *background-only* hypotheses. The limits are determined using the CL_s method [73, 74] and the procedure is described in Ref. [75, 76].

Systematic uncertainties are taken into account as nuisance parameters in the fit procedure: normalisation uncertainties affect the signal and background yields. Uncertainties on the τ

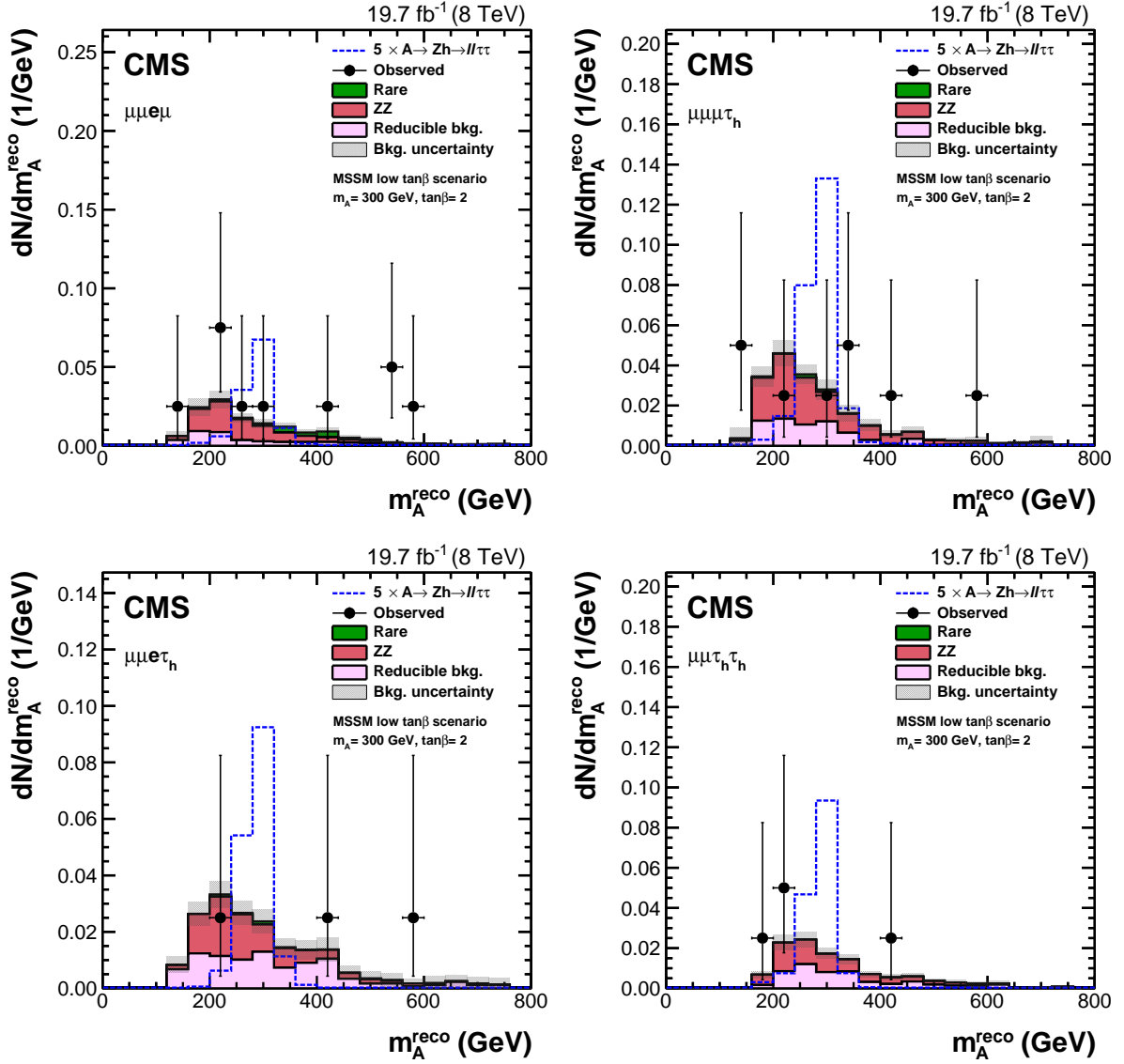


Figure 7: Invariant mass distributions for different final states of the $A \rightarrow Zh$ process where Z decays to $\mu\mu$. The expected signal scaled by a factor 5 is shown superimposed as an open dashed histogram for $\tan\beta = 2$ and $m_A = 300 \text{ GeV}$ in the low $\tan\beta$ scenario of MSSM. Expected background contributions are shown for the values of nuisance parameters (systematic uncertainties) obtained after fitting the signal plus background hypothesis to the data.

energy scale and jet energy scale are propagated as shape uncertainties.

The model independent expected and observed cross section times branching fraction limits for the $H \rightarrow hh \rightarrow bb\tau\tau$ process are shown in Fig. 8 and for the $A \rightarrow Zh \rightarrow LL\tau\tau$ process in Figs. 9 and 10 where $L = e, \mu$ or τ in order to reflect the small $Z \rightarrow \tau\tau$ contribution to the signal acceptance.

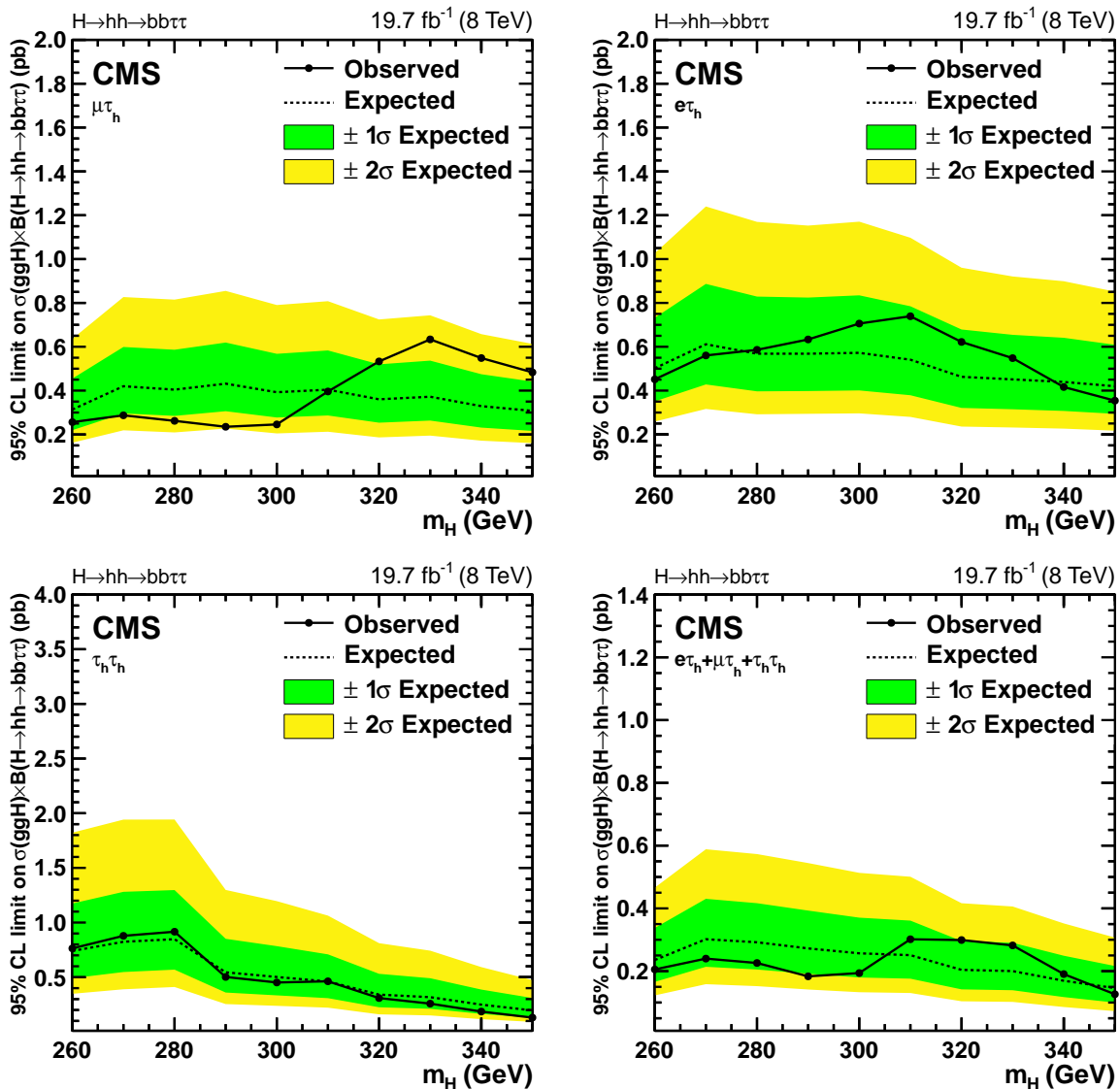


Figure 8: Upper limits at 95% CL on the $H \rightarrow hh \rightarrow bb\tau\tau$ cross section times branching fraction for the $\mu\tau_h$ (top left), $e\tau_h$ (top right), $\tau_h\tau_h$ (bottom left), and for final states combined (bottom right)

We interpret the observed limits on the cross section times branching fraction in the MSSM and 2HDM frameworks, discussed in Section 1.

In the MSSM we interpret them in the “low $\tan\beta$ ” scenario [27, 77] in which the value of M_{SUSY} is increased until the mass of the lightest Higgs boson is consistent with 125 GeV over a range of low $\tan\beta$ and m_A values. The exclusion region in the m_A - $\tan\beta$ plane for the combination of the $H \rightarrow hh \rightarrow bb\tau\tau$ and $A \rightarrow Zh \rightarrow \ell\ell\tau\tau$ analyses, in such a scenario, is shown in Fig. 11. The limit falls off rapidly as m_A approaches 350 GeV because decays of the A to two top quarks

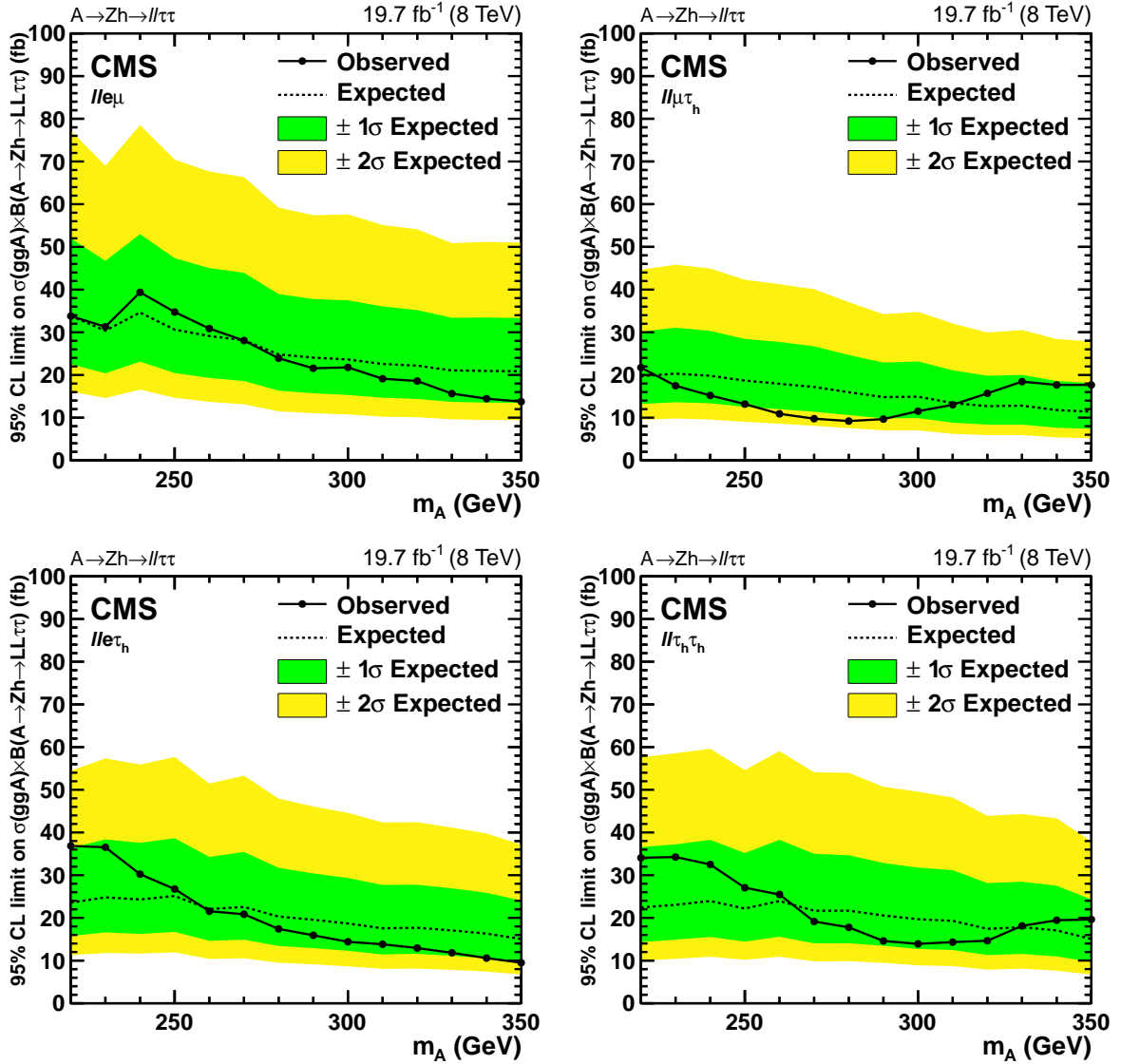


Figure 9: Upper limits at 95% CL on cross section times branching fraction on $A \rightarrow \text{Zh} \rightarrow \text{LL}\tau\tau$ for $lle\mu$ (top left), $ll\mu\tau_h$ (top right), $lle\tau_h$ (bottom left), and $ll\tau_h\tau_h$ (bottom right) final states.

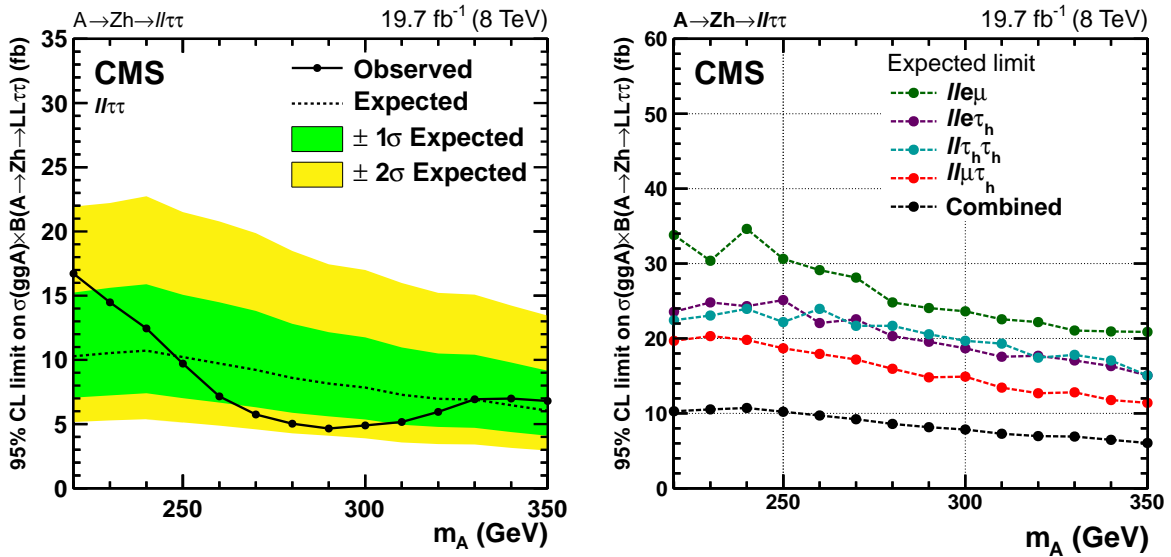


Figure 10: Upper limits at 95% CL on cross section times branching fraction on $A \rightarrow Zh \rightarrow LL\tau\tau$ for all $\ell\ell\tau\tau$ final states combined (left) and comparison of the different final states (right).

are becoming kinematically allowed.

The interpretation of the observed limits in a Type II 2HDM is performed in the “physics basis”. The inputs to this interpretation are the physical Higgs boson masses (m_h, m_H, m_A, m_{H^\pm}), the ratio of the vacuum expectation energies ($\tan\beta$), the CP-even Higgs mixing angle (α) and $m_{12}^2 = m_A^2 [\tan\beta / (1 + \tan\beta^2)]$. For simplicity we assume that $m_H = m_A = m_{H^\pm}$.

The cross-sections and branching fractions in the 2HDM were calculated as described by the LHC Higgs Cross Section Working Group [77, 78]. The exclusion regions, calculated using the combination of the $H \rightarrow hh \rightarrow bb\tau\tau$ and $A \rightarrow Zh \rightarrow \ell\ell\tau\tau$ analyses, in the $\cos(\beta - \alpha)$ vs. $\tan\beta$ plane for such a Type II 2HDM scenario with a heavy Higgs boson mass of 300 GeV are shown in Fig. 12. This can be compared to Fig. 5 in Ref. [41].

8 Summary

A search for a heavy scalar Higgs boson (H) decaying into a pair of SM-like Higgs bosons (hh) and a search for a heavy neutral pseudoscalar Higgs boson (A) decaying into a Z boson and a SM-like Higgs boson (h), have been performed using events recorded by the CMS experiment at the LHC. The dataset corresponds to an integrated luminosity of 19.7 fb^{-1} , recorded at 8 TeV centre-of-mass energy in 2012. No evidence for a signal has been found and exclusion limits on the production cross section times branching fraction for the processes $H \rightarrow hh \rightarrow bb\tau\tau$ and $A \rightarrow Zh \rightarrow LL\tau\tau$ are presented. The results are also interpreted in the context of the MSSM and 2HDM models.

Acknowledgments

We congratulate our colleagues in the CERN accelerator departments for the excellent performance of the LHC and thank the technical and administrative staffs at CERN and at other CMS institutes for their contributions to the success of the CMS effort. In addition, we gratefully acknowledge the computing centres and personnel of the Worldwide LHC Computing Grid for delivering so effectively the computing infrastructure essential to our analyses. Finally, we

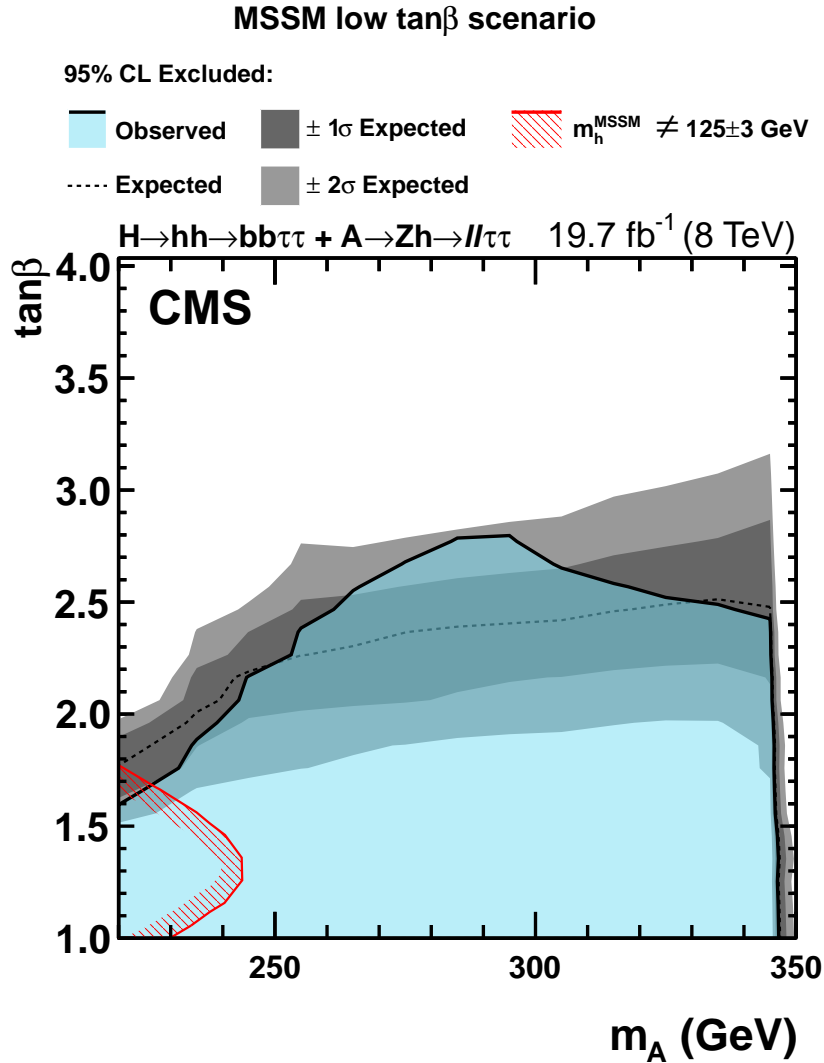


Figure 11: The 95% CL exclusion region in the m_A - $\tan\beta$ plane for the low- $\tan\beta$ scenario as discussed in the introduction, combining the results of the $H \rightarrow hh \rightarrow bb\tau\tau$ and the $A \rightarrow Zh \rightarrow \ell\ell\tau\tau$ analysis. The area highlighted in blue below the black curve marks the observed exclusion. The dashed curve and the grey bands show the expected exclusion limit with the relative uncertainty. The red area with the back-slash lines at the lower-left corner of the plot indicates the region excluded by the mass of the SM-like scalar boson being 125 GeV. The limit falls off rapidly as m_A approaches 350 GeV because decays of the A to two top quarks are becoming kinematically allowed.

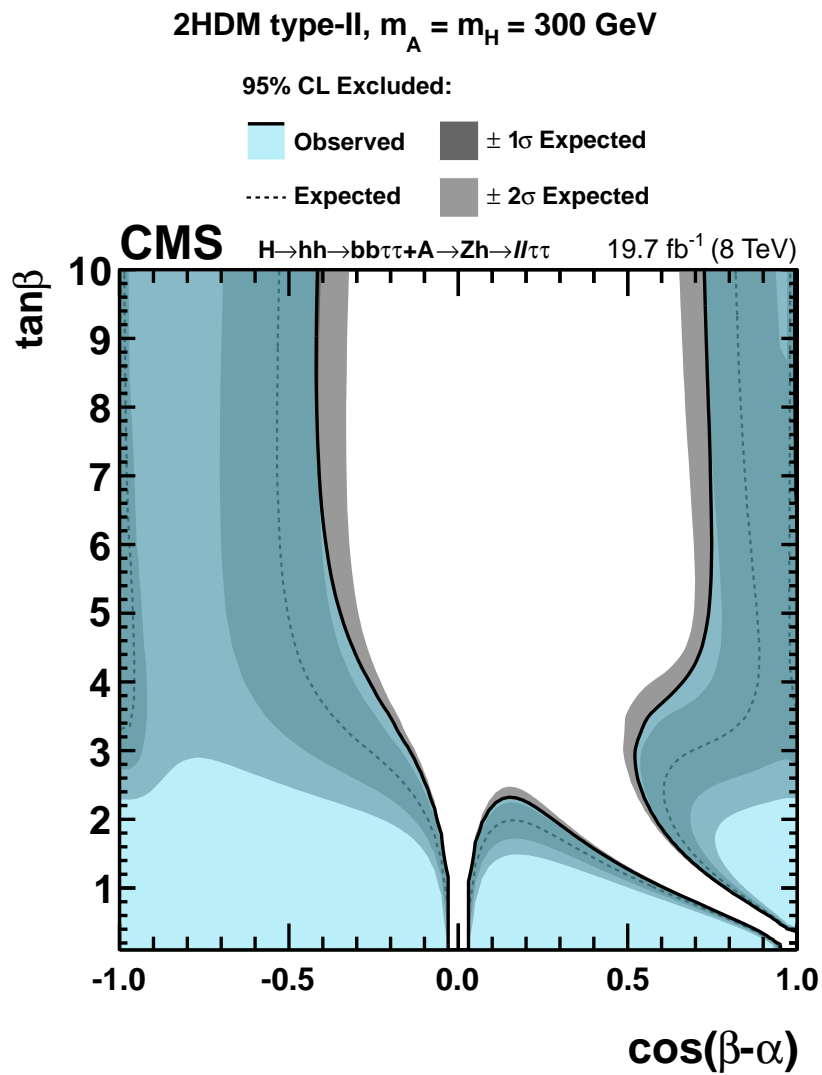


Figure 12: The 95% CL exclusion regions in the $\cos(\beta - \alpha)$ vs. $\tan \beta$ plane of 2HDM Type II model for $m_A = m_H = 300$ GeV, combining the results of the $H \rightarrow hh \rightarrow bb\tau\tau$ and $A \rightarrow Zh \rightarrow \ell\ell\tau\tau$ analysis. The areas highlighted in blue bounded by the black curves mark the observed exclusion. The dashed curves and the grey bands show the expected exclusion limit with the relative uncertainty.

acknowledge the enduring support for the construction and operation of the LHC and the CMS detector provided by the following funding agencies: BMWFW and FWF (Austria); FNRS and FWO (Belgium); CNPq, CAPES, FAPERJ, and FAPESP (Brazil); MES (Bulgaria); CERN; CAS, MoST, and NSFC (China); COLCIENCIAS (Colombia); MSES and CSF (Croatia); RPF (Cyprus); MoER, ERC IUT and ERDF (Estonia); Academy of Finland, MEC, and HIP (Finland); CEA and CNRS/IN2P3 (France); BMBF, DFG, and HGF (Germany); GSRT (Greece); OTKA and NIH (Hungary); DAE and DST (India); IPM (Iran); SFI (Ireland); INFN (Italy); MSIP and NRF (Republic of Korea); LAS (Lithuania); MOE and UM (Malaysia); CINVESTAV, CONACYT, SEP, and UASLP-FAI (Mexico); MBIE (New Zealand); PAEC (Pakistan); MSHE and NSC (Poland); FCT (Portugal); JINR (Dubna); MON, RosAtom, RAS and RFBR (Russia); MESTD (Serbia); SEIDI and CPAN (Spain); Swiss Funding Agencies (Switzerland); MST (Taipei); ThEPCenter, IPST, STAR and NSTDA (Thailand); TUBITAK and TAEK (Turkey); NASU and SFFR (Ukraine); STFC (United Kingdom); DOE and NSF (USA).

Individuals have received support from the Marie-Curie programme and the European Research Council and EPLANET (European Union); the Leventis Foundation; the A. P. Sloan Foundation; the Alexander von Humboldt Foundation; the Belgian Federal Science Policy Office; the Fonds pour la Formation à la Recherche dans l'Industrie et dans l'Agriculture (FRIA-Belgium); the Agentschap voor Innovatie door Wetenschap en Technologie (IWT-Belgium); the Ministry of Education, Youth and Sports (MEYS) of the Czech Republic; the Council of Science and Industrial Research, India; the HOMING PLUS programme of the Foundation for Polish Science, cofinanced from European Union, Regional Development Fund; the OPUS programme of the National Science Center (Poland); the Compagnia di San Paolo (Torino); the Consorzio per la Fisica (Trieste); MIUR project 20108T4XTM (Italy); the Thalís and Aristeia programmes cofinanced by EU-ESF and the Greek NSRF; the National Priorities Research Program by Qatar National Research Fund; the Rachadapisek Sompot Fund for Postdoctoral Fellowship, Chulalongkorn University (Thailand); and the Welch Foundation, contract C-1845.

References

- [1] S. L. Glashow and S. Weinberg, "Natural conservation laws for neutral currents", *Phys. Rev. D* **15** (1977) 1958, doi:10.1103/PhysRevD.15.1958.
- [2] J. F. Gunion, H. E. Haber, G. Kane, and S. Dawson, "The Higgs Hunter's Guide". Addison-Wesley, 2000. [Frontiers in Physics, 80].
- [3] G. C. Branco et al., "Theory and phenomenology of two-Higgs-doublet models", *Phys. Rept.* **516** (2012) 1, doi:10.1016/j.physrep.2012.02.002, arXiv:1106.0034.
- [4] P. Fayet, "Supergauge invariant extension of the Higgs mechanism and a model for the electron and its neutrino", *Nucl. Phys. B* **90** (1975) 104, doi:10.1016/0550-3213(75)90636-7.
- [5] P. Fayet, "Supersymmetry and weak, electromagnetic and strong interactions", *Phys. Lett. B* **64** (1976) 159, doi:10.1016/0370-2693(76)90319-1.
- [6] P. Fayet, "Spontaneously broken supersymmetric theories of weak, electromagnetic and strong interactions", *Phys. Lett. B* **69** (1977) 489, doi:10.1016/0370-2693(77)90852-8.
- [7] S. Dimopoulos and H. Georgi, "Softly broken supersymmetry and SU(5)", *Nucl. Phys. B* **193** (1981) 150, doi:10.1016/0550-3213(81)90522-8.
- [8] N. Sakai, "Naturalness in supersymmetric GUTS", *Z. Phys. C* **11** (1981) 153, doi:10.1007/BF01573998.
- [9] K. Inoue, A. Kakuto, H. Komatsu, and S. Takeshita, "Low-Energy Parameters and Particle Masses in a Supersymmetric Grand Unified Model", *Prog. Theor. Phys.* **67** (1982) 1889, doi:10.1143/PTP.67.1889.
- [10] K. Inoue, A. Kakuto, H. Komatsu, and S. Takeshita, "Aspects of Grand Unified Models with Softly Broken Supersymmetry", *Prog. Theor. Phys.* **68** (1982) 927, doi:10.1143/PTP.68.927.
- [11] K. Inoue, A. Kakuto, H. Komatsu, and S. Takeshita, "Renormalization of Supersymmetry Breaking Parameters Revisited", *Prog. Theor. Phys.* **71** (1984) 413, doi:10.1143/PTP.71.413.
- [12] A. Djouadi, "The anatomy of electroweak symmetry breaking Tome II: The Higgs bosons in the Minimal Supersymmetric Model", *Phys. Rept.* **459** (2008) 1, doi:10.1016/j.physrep.2007.10.005, arXiv:hep-ph/0503173.
- [13] Y. Okada, M. Yamaguchi, and T. Yanagida, "Upper Bound of the Lightest Higgs Boson Mass in the Minimal Supersymmetric Standard Model", *Prog. Theor. Phys.* **85** (1991) 1, doi:10.1143/PTP/85.1.1.
- [14] J. R. Ellis, G. Ridolfi, and F. Zwirner, "Radiative corrections to the masses of supersymmetric Higgs bosons", *Phys. Lett. B* **257** (1991) 83, doi:10.1016/0370-2693(91)90863-L.
- [15] H. E. Haber and R. Hempfling, "Can the Mass of the Lightest Higgs Boson of the Minimal Supersymmetric Model be Larger than m_Z ?", *Phys. Rev. Lett.* **66** (1991) 1815, doi:10.1103/PhysRevLett.66.1815.

- [16] M. Carena, J. R. Espinosa, M. Quiros, and C. E. M. Wagner, "Analytical expressions for radiatively corrected Higgs masses and couplings in the MSSM", *Phys. Lett. B* **355** (1995) 209, doi:10.1016/0370-2693(95)00694-G, arXiv:hep-ph/9504316.
- [17] M. Carena, D. Garcia, U. Nierste, and C. E. M. Wagner, "Effective Lagrangian for the $\bar{t}bH^+$ interaction in the MSSM and charged Higgs phenomenology", *Nucl. Phys. B* **577** (2000) 88, doi:10.1016/S0550-3213(00)00146-2, arXiv:hep-ph/9912516.
- [18] CMS Collaboration, "Search for neutral MSSM Higgs bosons decaying to a pair of tau leptons in pp collisions", *JHEP* **10** (2014) 160, doi:10.1007/JHEP10(2014)160, arXiv:1408.3316.
- [19] CMS Collaboration, "Search for neutral MSSM Higgs bosons decaying into a pair of bottom quarks", (2015). arXiv:1506.08329.
- [20] ATLAS Collaboration, "Search for neutral Higgs bosons of the minimal supersymmetric standard model in pp collisions at $\sqrt{s} = 8$ TeV with the ATLAS detector", *JHEP* **11** (2014) 056, doi:10.1007/JHEP11(2014)056, arXiv:1409.6064.
- [21] M. S. Carena et al., "MSSM Higgs boson searches at the LHC: benchmark scenarios after the discovery of a Higgs-like particle", *Eur. Phys. J. C* **73** (2013) 2552, doi:10.1140/epjc/s10052-013-2552-1, arXiv:1302.7033.
- [22] ATLAS and CMS Collaboration, "Combined Measurement of the Higgs Boson Mass in pp Collisions at $\sqrt{s} = 7$ and 8 TeV with the ATLAS and CMS Experiments", *Phys. Rev. Lett.* **114** (2015) 191803, doi:10.1103/PhysRevLett.114.191803, arXiv:1503.07589.
- [23] A. Djouadi and J. Quevillon, "The MSSM Higgs sector at a high M_{SUSY} : reopening the low $\tan\beta$ regime and heavy Higgs searches", *JHEP* **10** (2013) 028, doi:10.1007/JHEP10(2013)028, arXiv:1304.1787.
- [24] M. Carena et al., "Complementarity between nonstandard Higgs boson searches and precision Higgs boson measurements in the MSSM", *Phys. Rev. D* **91** (2015) 035003, doi:10.1103/PhysRevD.91.035003, arXiv:1410.4969.
- [25] A. Djouadi et al., "The post-Higgs MSSM scenario: habemus MSSM?", *Eur. Phys. J. C* **73** (2013) 2650, doi:10.1140/epjc/s10052-013-2650-0, arXiv:1307.5205.
- [26] A. Djouadi et al., "Fully covering the MSSM Higgs sector at the LHC", (2015). arXiv:1502.05653.
- [27] E. Bagnaschi et al., "Benchmark scenarios for low $\tan\beta$ in the MSSM", Technical Report LHCHXSWG-2015-002, CERN, Geneva, Aug, 2015.
- [28] A. Arbey, M. Battaglia, and F. Mahmoudi, "Supersymmetric heavy Higgs bosons at the LHC", *Phys. Rev. D* **88** (2013) 015007, doi:10.1103/PhysRevD.88.015007, arXiv:1303.7450.
- [29] ATLAS Collaboration, "Observation of a new particle in the search for the Standard Model Higgs boson with the ATLAS detector at the LHC", *Phys. Lett. B* **716** (2012) 1, doi:10.1016/j.physletb.2012.08.020, arXiv:1207.7214.
- [30] CMS Collaboration, "Observation of a new boson at a mass of 125 GeV with the CMS experiment at the LHC", *Phys. Lett. B* **716** (2012) 30, doi:10.1016/j.physletb.2012.08.021, arXiv:1207.7235.

- [31] CMS Collaboration, “Observation of a new boson with mass near 125 GeV in pp collisions at $\sqrt{s} = 7$ and 8 TeV”, *JHEP* **06** (2013) 081, doi:10.1007/JHEP06(2013)081, arXiv:1303.4571.
- [32] D. M. Asner et al., “ILC Higgs White Paper”, (2013). arXiv:1310.0763.
- [33] CMS Collaboration, “Evidence for the direct decay of the 125 GeV Higgs boson to fermions”, *Nature Phys.* **10** (2014) 557, doi:10.1038/nphys3005, arXiv:1401.6527.
- [34] CMS Collaboration, “Evidence for the 125 GeV Higgs boson decaying to a pair of τ leptons”, *JHEP* **05** (2014) 104, doi:10.1007/JHEP05(2014)104, arXiv:1401.5041.
- [35] ATLAS Collaboration, “Search For Higgs Boson Pair Production in the $\gamma\gamma b\bar{b}$ Final State using pp Collision Data at $\sqrt{s} = 8$ TeV from the ATLAS Detector”, *Phys. Rev. Lett.* **114** (2015) 081802, doi:10.1103/PhysRevLett.114.081802, arXiv:1406.5053.
- [36] ATLAS Collaboration, “Search for a CP-odd Higgs boson decaying to Zh in pp collisions at $\sqrt{s} = 8$ TeV with the ATLAS detector”, *Phys. Lett. B* **744** (2015) 163, doi:10.1016/j.physletb.2015.03.054, arXiv:1502.04478.
- [37] ATLAS Collaboration, “Search for Higgs boson pair production in the $b\bar{b}b\bar{b}$ final state from pp collisions at $\sqrt{s} = 8$ TeV with the ATLAS detector”, *Eur. Phys. J. C* (2015), no. 75, 412, doi:10.1140/epjc/s10052-015-3628-x, arXiv:1506.00285.
- [38] ATLAS Collaboration, “Searches for Higgs boson pair production in the $hh \rightarrow bb\tau\tau, \gamma\gamma WW^*, \gamma\gamma bb, bbbb$ channels with the ATLAS detector”, *Phys. Rev. D* **92** (2015), no. 9, 092004, doi:10.1103/PhysRevD.92.092004, arXiv:1509.04670.
- [39] CMS Collaboration, “Searches for heavy Higgs bosons in two-Higgs-doublet models and for $t \rightarrow ch$ decay using multilepton and diphoton final states in pp collisions at 8 TeV”, *Phys. Rev. D* **90** (2014) 112013, doi:10.1103/PhysRevD.90.112013, arXiv:1410.2751.
- [40] CMS Collaboration, “Search for resonant pair production of Higgs bosons decaying to two bottom quark-antiquark pairs in proton-proton collisions at 8 TeV”, (2015). arXiv:1503.04114.
- [41] CMS Collaboration, “Search for a pseudoscalar boson decaying into a Z boson and the 125 GeV Higgs boson in $l^+l^- b\bar{b}$ final states”, (2015). arXiv:1504.04710.
- [42] CMS Collaboration, “The CMS experiment at the CERN LHC”, *JINST* **3** (2008) S08004, doi:10.1088/1748-0221/3/08/S08004.
- [43] T. Sjöstrand, S. Mrenna, and P. Z. Skands, “PYTHIA 6.4 physics and manual”, *JHEP* **05** (2006) 026, doi:10.1088/1126-6708/2006/05/026, arXiv:hep-ph/0603175.
- [44] J. Alwall et al., “MadGraph 5: going beyond”, *JHEP* **06** (2011) 128, doi:10.1007/JHEP06(2011)128, arXiv:1106.0522.
- [45] P. Nason, “A New method for combining NLO QCD with shower Monte Carlo algorithms”, *JHEP* **11** (2004) 040, doi:10.1088/1126-6708/2004/11/040, arXiv:hep-ph/0409146.
- [46] S. Frixione, P. Nason, and C. Oleari, “Matching NLO QCD computations with parton shower simulations: the POWHEG method”, *JHEP* **11** (2007) 070, doi:10.1088/1126-6708/2007/11/070, arXiv:0709.2092.

- [47] S. Alioli, P. Nason, C. Oleari, and E. Re, “NLO single-top production matched with shower in POWHEG: s - and t -channel contributions”, *JHEP* **09** (2009) 111, doi:10.1088/1126-6708/2009/09/111, arXiv:0907.4076. [Erratum: doi:10.1007/JHEP02(2010)011].
- [48] S. Alioli, P. Nason, C. Oleari, and E. Re, “A general framework for implementing NLO calculations in shower Monte Carlo programs: the POWHEG BOX”, *JHEP* **06** (2010) 043, doi:10.1007/JHEP06(2010)043, arXiv:1002.2581.
- [49] CMS Collaboration, “Jet and underlying event properties as a function of charged-particle multiplicity in proton-proton collisions at $\sqrt{s} = 7$ TeV”, *Eur. Phys. J. C* **73** (2013) 2674, doi:10.1140/epjc/s10052-013-2674-5, arXiv:1310.4554.
- [50] N. Davidson et al., “Universal interface of TAUOLA: Technical and physics documentation”, *Comput. Phys. Commun.* **183** (2012) 821, doi:10.1016/j.cpc.2011.12.009, arXiv:1002.0543.
- [51] GEANT4 Collaboration, “GEANT4 — a simulation toolkit”, *Nucl. Instrum. Meth. A* **506** (2003) 250, doi:10.1016/S0168-9002(03)01368-8.
- [52] H.-L. Lai et al., “New parton distributions for collider physics”, *Phys. Rev. D* **82** (2010) 074024, doi:10.1103/PhysRevD.82.074024, arXiv:1007.2241.
- [53] J. Pumplin et al., “New generation of parton distributions with uncertainties from global QCD analysis”, *JHEP* **07** (2002) 012, doi:10.1088/1126-6708/2002/07/012, arXiv:hep-ph/0201195.
- [54] A. D. Martin, W. J. Stirling, R. S. Thorne, and G. Watt, “Parton distributions for the LHC”, *Eur. Phys. J. C* **63** (2009) 189, doi:10.1140/epjc/s10052-009-1072-5, arXiv:0901.0002.
- [55] M. Botje et al., “The PDF4LHC Working Group Interim Recommendations”, (2011). arXiv:1101.0538.
- [56] CMS Collaboration, “Particle-Flow Event Reconstruction in CMS and Performance for Jets, Taus, and E_T^{miss} ”, CMS Physics Analysis Summary CMS-PAS-PFT-09-001, 2009.
- [57] CMS Collaboration, “Commissioning of the Particle-flow Event Reconstruction with the first LHC collisions recorded in the CMS detector”, CMS Physics Analysis Summary CMS-PAS-PFT-10-001, 2010.
- [58] CMS Collaboration, “Performance of CMS muon reconstruction in pp collision events at $\sqrt{s} = 7$ TeV”, *JINST* **7** (2012) P10002, doi:10.1088/1748-0221/7/10/P10002, arXiv:1206.4071.
- [59] CMS Collaboration, “Performance of electron reconstruction and selection with the CMS detector in proton-proton collisions at $\sqrt{s} = 8$ TeV”, *JINST* **10** (2015) P06005, doi:10.1088/1748-0221/10/06/P06005, arXiv:1502.02701.
- [60] CMS Collaboration, “The performance of the CMS muon detector in proton-proton collisions at $\sqrt{s} = 7$ TeV at the LHC”, *JINST* **8** (2013) P11002, doi:10.1088/1748-0221/8/11/P11002, arXiv:1306.6905.

- [61] CMS Collaboration, “Measurements of inclusive W and Z cross sections in pp collisions at $\sqrt{s} = 7$ TeV”, *JHEP* **01** (2011) 080, doi:10.1007/JHEP01(2011)080, arXiv:1012.2466.
- [62] M. Cacciari, G. P. Salam, and G. Soyez, “FastJet user manual”, *Eur. Phys. J. C* **72** (2012) 1896, doi:10.1140/epjc/s10052-012-1896-2, arXiv:1111.6097.
- [63] M. Cacciari and G. P. Salam, “Dispelling the N^3 myth for the k_t jet-finder”, *Phys. Lett. B* **641** (2006) 57, doi:10.1016/j.physletb.2006.08.037, arXiv:hep-ph/0512210.
- [64] M. Cacciari and G. P. Salam, “Pileup subtraction using jet areas”, *Phys. Lett. B* **659** (2008) 119, doi:10.1016/j.physletb.2007.09.077, arXiv:0707.1378.
- [65] CMS Collaboration, “Pileup Jet Identification”, CMS Physics Analysis Summary CMS-PAS-JME-13-005, 2013.
- [66] CMS Collaboration, “Performance of the CMS missing transverse momentum reconstruction in pp data at $\sqrt{s} = 8$ TeV”, *JINST* **10** (2015) P02006, doi:10.1088/1748-0221/10/02/P02006, arXiv:1411.0511.
- [67] CMS Collaboration, “Identification of b-quark jets with the CMS experiment”, *JINST* **8** (2013) P04013, doi:10.1088/1748-0221/8/04/P04013, arXiv:1211.4462.
- [68] CMS Collaboration, “Reconstruction and identification of lepton decays to hadrons and at CMS”, *JINST* **11** (2016), no. 01, P01019, doi:10.1088/1748-0221/11/01/P01019, arXiv:1510.07488.
- [69] CMS Collaboration, “Measurement of the inclusive Z cross section via decays to tau pairs in pp collisions at $\sqrt{s} = 7$ TeV”, *JHEP* **08** (2011) 117, doi:10.1007/JHEP08(2011)117, arXiv:1104.1617.
- [70] CMS Collaboration, “CMS Luminosity Based on Pixel Cluster Counting — Summer 2013 Update”, CMS Physics Analysis Summary CMS-PAS-LUM-13-001, 2013.
- [71] CMS Collaboration, “Determination of Jet Energy Calibration and Transverse Momentum Resolution in CMS”, *JINST* **6** (2011) P11002, doi:10.1088/1748-0221/6/11/P11002, arXiv:1107.4277.
- [72] L. Bianchini, J. Conway, E. K. Friis, and C. Veelken, “Reconstruction of the Higgs mass in $H \rightarrow \tau\tau$ Events by Dynamical Likelihood techniques”, *J. Phys. Conf. Ser.* **513** (2014) 022035, doi:10.1088/1742-6596/513/2/022035.
- [73] T. Junk, “Confidence level computation for combining searches with small statistics”, *Nucl. Instrum. Meth. A* **434** (1999) 435, doi:10.1016/S0168-9002(99)00498-2, arXiv:hep-ex/9902006.
- [74] A. L. Read, “Presentation of search results: The CL_s technique”, *J. Phys. G* **28** (2002) 2693, doi:10.1088/0954-3899/28/10/313.
- [75] ATLAS and CMS, LHC Higgs Combination Group, “Procedure for the LHC Higgs boson search combination in Summer 2011”, Technical Report ATL-PHYS-PUB 2011-11, CMS NOTE 2011/005, CERN, 2011.

-
- [76] G. Cowan, K. Cranmer, E. Gross, and O. Vitells, “Asymptotic formulae for likelihood-based tests of new physics”, *Eur. Phys. J. C* **71** (2011) 1554, doi:10.1140/epjc/s10052-011-1554-0, arXiv:1007.1727. [Erratum: doi:10.1140/epjc/s10052-013-2501-z].
- [77] R. V. Harlander, S. Liebler, and H. Mantler, “SusHi: A program for the calculation of Higgs production in gluon fusion and bottom-quark annihilation in the Standard Model and the MSSM”, *Comput. Phys. Commun.* **184** (2013) 1605, doi:10.1016/j.cpc.2013.02.006, arXiv:1212.3249.
- [78] R. Harlander et al., “Interim recommendations for the evaluation of Higgs production cross sections and branching ratios at the LHC in the Two-Higgs-Doublet Model”, (2013). arXiv:1312.5571.

A Kinematic Fit

In the analysed event topology $H \rightarrow hh \rightarrow bb\tau\tau$, the collinear approximation for the decay products of the τ leptons is assumed. This is well motivated, since the τ leptons are highly boosted as they originate from a relatively heavy object compared to their own mass, $m_h/m_\tau = 70$. Further, it is assumed that the reconstruction of the directions of all final state objects η_i and ϕ_i with $i \in \{b_1, b_2, \tau_1^{\text{vis}}, \tau_2^{\text{vis}}\}$ is accurate and the uncertainties can be neglected compared to the uncertainties on the energy reconstruction.

Both, the pair of b jets and the pair of τ leptons need to fulfil an invariant mass constraint

$$m(\tau_1, \tau_2) = m(b_1, b_2) = m_h = 125 \text{ GeV}. \quad (2)$$

These two hard constraints reduce the number of fit parameters to two, chosen to be E_{b_1} and E_{τ_1} .

For the two measured b jet energies, the χ^2 terms can be formulated as

$$\chi_{b_{1,2}}^2 = \left(\frac{E_{b_{1,2}}^{\text{fit}} - E_{b_{1,2}}^{\text{meas}}}{\sigma_{b_{1,2}}} \right)^2, \quad (3)$$

where $E_{b_{1,2}}^{\text{fit}}$ are the fitted and $E_{b_{1,2}}^{\text{meas}}$ are the reconstructed b jet energy, and $\sigma_{b_{1,2}}$ describe the b jet energy resolution.

In the decay of the two τ leptons at least two neutrinos are involved. Thus there exists no good measurement of the original τ lepton energies, but only lower energy limits. For this reason, the τ lepton energies are constrained from the balance of the fitted heavy Higgs boson transverse momentum

$$\vec{p}_{T,H}^{\text{fit}} = \vec{p}_{T,b_1}^{\text{fit}} + \vec{p}_{T,b_2}^{\text{fit}} + \vec{p}_{T,\tau_1}^{\text{fit}} + \vec{p}_{T,\tau_2}^{\text{fit}} \quad (4)$$

and the reconstructed transversal recoil

$$\vec{p}_{T,\text{recoil}}^{\text{meas}} = -\vec{p}_{T,\text{miss}}^{\text{meas}} - \vec{p}_{T,b_1}^{\text{meas}} - \vec{p}_{T,b_2}^{\text{meas}} - \vec{p}_{T,\tau_1^{\text{vis}}}^{\text{meas}} - \vec{p}_{T,\tau_2^{\text{vis}}}^{\text{meas}} = -\vec{p}_{T,H}^{\text{meas}}. \quad (5)$$

Herein, $\vec{p}_{T,\text{miss}}^{\text{meas}}$ denotes the reconstructed missing momentum in the transverse plane, which has been determined from E_T^{miss} reconstruction algorithms, as described in Sec. 3. Any nonzero residual vector $\vec{p}_{T,\text{recoil}}^{\text{res}} = \vec{p}_{T,H}^{\text{fit}} + \vec{p}_{T,\text{recoil}}^{\text{meas}}$ contributes to a χ^2 term as follows

$$\chi_{\text{recoil}}^2 = \vec{p}_{T,\text{recoil}}^{\text{res},T} \cdot V_{\text{recoil}}^{-1} \cdot \vec{p}_{T,\text{recoil}}^{\text{res}}, \quad (6)$$

where V_{recoil} denotes the covariance matrix of the reconstructed recoil vector.

The overall χ^2 function finally reads,

$$\chi^2 = \chi_{b_1}^2 + \chi_{b_2}^2 + \chi_{\text{recoil}}^2. \quad (7)$$

After minimisation of this function by varying E_{b_1} and E_{τ_1} , a very accurate reconstruction of the heavy Higgs boson mass (M_H^{kinfit}) is achieved.

B The CMS Collaboration

Yerevan Physics Institute, Yerevan, Armenia

V. Khachatryan, A.M. Sirunyan, A. Tumasyan

Institut für Hochenergiephysik der OeAW, Wien, Austria

W. Adam, E. Asilar, T. Bergauer, J. Brandstetter, E. Brondolin, M. Dragicevic, J. Erö, M. Flechl, M. Friedl, R. Frühwirth¹, V.M. Ghete, C. Hartl, N. Hörmann, J. Hrubec, M. Jeitler¹, V. Knünz, A. König, M. Krammer¹, I. Krätschmer, D. Liko, T. Matsushita, I. Mikulec, D. Rabady², B. Rahbaran, H. Rohringer, J. Schieck¹, R. Schöfbeck, J. Strauss, W. Treberer-Treberspurg, W. Waltenberger, C.-E. Wulz¹

National Centre for Particle and High Energy Physics, Minsk, Belarus

V. Mossolov, N. Shumeiko, J. Suarez Gonzalez

Universiteit Antwerpen, Antwerpen, Belgium

S. Alderweireldt, T. Cornelis, E.A. De Wolf, X. Janssen, A. Knutsson, J. Lauwers, S. Luyckx, S. Ochesanu, R. Rougny, M. Van De Klundert, H. Van Haevermaet, P. Van Mechelen, N. Van Remortel, A. Van Spilbeek

Vrije Universiteit Brussel, Brussel, Belgium

S. Abu Zeid, F. Blekman, J. D'Hondt, N. Daci, I. De Bruyn, K. Deroover, N. Heracleous, J. Keaveney, S. Lowette, L. Moreels, A. Olbrechts, Q. Python, D. Strom, S. Tavernier, W. Van Doninck, P. Van Mulders, G.P. Van Onsem, I. Van Parijs

Université Libre de Bruxelles, Bruxelles, Belgium

P. Barria, H. Brun, C. Caillol, B. Clerbaux, G. De Lentdecker, H. Delannoy, G. Fasanella, L. Favart, A.P.R. Gay, A. Grebenyuk, G. Karapostoli, T. Lenzi, A. Léonard, T. Maerschalk, A. Marinov, L. Perniè, A. Randle-conde, T. Reis, T. Seva, C. Vander Velde, P. Vanlaer, R. Yonamine, F. Zenoni, F. Zhang³

Ghent University, Ghent, Belgium

K. Beernaert, L. Benucci, A. Cimmino, S. Crucy, D. Dobur, A. Fagot, G. Garcia, M. Gul, J. Mccartin, A.A. Ocampo Rios, D. Poyraz, D. Ryckbosch, S. Salva, M. Sigamani, N. Strobbe, M. Tytgat, W. Van Driessche, E. Yazgan, N. Zaganidis

Université Catholique de Louvain, Louvain-la-Neuve, Belgium

S. Basegmez, C. Beluffi⁴, O. Bondu, S. Brochet, G. Bruno, R. Castello, A. Caudron, L. Ceard, G.G. Da Silveira, C. Delaere, D. Favart, L. Forthomme, A. Giammanco⁵, J. Hollar, A. Jafari, P. Jez, M. Komm, V. Lemaitre, A. Mertens, C. Nuttens, L. Perrini, A. Pin, K. Piotrkowski, A. Popov⁶, L. Quertenmont, M. Selvaggi, M. Vidal Marono

Université de Mons, Mons, Belgium

N. Belyi, G.H. Hammad

Centro Brasileiro de Pesquisas Fisicas, Rio de Janeiro, Brazil

W.L. Aldá Júnior, G.A. Alves, L. Brito, M. Correa Martins Junior, M. Hamer, C. Hensel, C. Mora Herrera, A. Moraes, M.E. Pol, P. Rebello Teles

Universidade do Estado do Rio de Janeiro, Rio de Janeiro, Brazil

E. Belchior Batista Das Chagas, W. Carvalho, J. Chinellato⁷, A. Custódio, E.M. Da Costa, D. De Jesus Damiao, C. De Oliveira Martins, S. Fonseca De Souza, L.M. Huertas Guativa, H. Malbouisson, D. Matos Figueiredo, L. Mundim, H. Nogima, W.L. Prado Da Silva, A. Santoro, A. Sznajder, E.J. Tonelli Manganote⁷, A. Vilela Pereira

Universidade Estadual Paulista ^a, Universidade Federal do ABC ^b, São Paulo, Brazil

S. Ahuja^a, C.A. Bernardes^b, A. De Souza Santos^b, S. Dogra^a, T.R. Fernandez Perez Tomei^a, E.M. Gregores^b, P.G. Mercadante^b, C.S. Moon^{a,8}, S.F. Novaes^a, Sandra S. Padula^a, D. Romero Abad, J.C. Ruiz Vargas

Institute for Nuclear Research and Nuclear Energy, Sofia, Bulgaria

A. Aleksandrov, R. Hadjiiska, P. Iaydjiev, M. Rodozov, S. Stoykova, G. Sultanov, M. Vutova

University of Sofia, Sofia, Bulgaria

A. Dimitrov, I. Glushkov, L. Litov, B. Pavlov, P. Petkov

Institute of High Energy Physics, Beijing, China

M. Ahmad, J.G. Bian, G.M. Chen, H.S. Chen, M. Chen, T. Cheng, R. Du, C.H. Jiang, R. Plestina⁹, F. Romeo, S.M. Shaheen, J. Tao, C. Wang, Z. Wang, H. Zhang

State Key Laboratory of Nuclear Physics and Technology, Peking University, Beijing, China

C. Asawatangtrakuldee, Y. Ban, Q. Li, S. Liu, Y. Mao, S.J. Qian, D. Wang, Z. Xu, W. Zou

Universidad de Los Andes, Bogota, Colombia

C. Avila, A. Cabrera, L.F. Chaparro Sierra, C. Florez, J.P. Gomez, B. Gomez Moreno, J.C. Sanabria

University of Split, Faculty of Electrical Engineering, Mechanical Engineering and Naval Architecture, Split, Croatia

N. Godinovic, D. Lelas, I. Puljak, P.M. Ribeiro Cipriano

University of Split, Faculty of Science, Split, Croatia

Z. Antunovic, M. Kovac

Institute Rudjer Boskovic, Zagreb, Croatia

V. Brigljevic, K. Kadija, J. Luetic, S. Micanovic, L. Sudic

University of Cyprus, Nicosia, Cyprus

A. Attikis, G. Mavromanolakis, J. Mousa, C. Nicolaou, F. Ptochos, P.A. Razis, H. Rykaczewski

Charles University, Prague, Czech Republic

M. Bodlak, M. Finger¹⁰, M. Finger Jr.¹⁰

Academy of Scientific Research and Technology of the Arab Republic of Egypt, Egyptian Network of High Energy Physics, Cairo, Egypt

A.A. Abdelalim^{11,12}, A. Awad, M. El Sawy^{13,14}, A. Mahrous¹¹, A. Radi^{14,15}

National Institute of Chemical Physics and Biophysics, Tallinn, Estonia

B. Calpas, M. Kadastik, M. Murumaa, M. Raidal, A. Tiko, C. Veelken

Department of Physics, University of Helsinki, Helsinki, Finland

P. Eerola, J. Pekkanen, M. Voutilainen

Helsinki Institute of Physics, Helsinki, Finland

J. Härkönen, V. Karimäki, R. Kinnunen, T. Lampén, K. Lassila-Perini, S. Lehti, T. Lindén, P. Luukka, T. Mäenpää, T. Peltola, E. Tuominen, J. Tuominiemi, E. Tuovinen, L. Wendland

Lappeenranta University of Technology, Lappeenranta, Finland

J. Talvitie, T. Tuuva

DSM/IRFU, CEA/Saclay, Gif-sur-Yvette, France

M. Besancon, F. Couderc, M. Dejardin, D. Denegri, B. Fabbro, J.L. Faure, C. Favaro, F. Ferri,

S. Ganjour, A. Givernaud, P. Gras, G. Hamel de Monchenault, P. Jarry, E. Locci, M. Machet, J. Malcles, J. Rander, A. Rosowsky, M. Titov, A. Zghiche

Laboratoire Leprince-Ringuet, Ecole Polytechnique, IN2P3-CNRS, Palaiseau, France

I. Antropov, S. Baffioni, F. Beaudette, P. Busson, L. Cadamuro, E. Chapon, C. Charlot, T. Dahms, O. Davignon, N. Filipovic, A. Florent, R. Granier de Cassagnac, S. Lisniak, L. Mastrolorenzo, P. Miné, I.N. Naranjo, M. Nguyen, C. Ochando, G. Ortona, P. Paganini, P. Pigard, S. Regnard, R. Salerno, J.B. Sauvan, Y. Sirois, T. Strebler, Y. Yilmaz, A. Zabi

Institut Pluridisciplinaire Hubert Curien, Université de Strasbourg, Université de Haute Alsace Mulhouse, CNRS/IN2P3, Strasbourg, France

J.-L. Agram¹⁶, J. Andrea, A. Aubin, D. Bloch, J.-M. Brom, M. Buttignol, E.C. Chabert, N. Chanon, C. Collard, E. Conte¹⁶, X. Coubez, J.-C. Fontaine¹⁶, D. Gelé, U. Goerlach, C. Goetzmann, A.-C. Le Bihan, J.A. Merlin², K. Skovpen, P. Van Hove

Centre de Calcul de l'Institut National de Physique Nucleaire et de Physique des Particules, CNRS/IN2P3, Villeurbanne, France

S. Gadrat

Université de Lyon, Université Claude Bernard Lyon 1, CNRS-IN2P3, Institut de Physique Nucléaire de Lyon, Villeurbanne, France

S. Beauceron, C. Bernet, G. Boudoul, E. Bouvier, C.A. Carrillo Montoya, R. Chierici, D. Contardo, B. Courbon, P. Depasse, H. El Mamouni, J. Fan, J. Fay, S. Gascon, M. Gouzevitch, B. Ille, F. Lagarde, I.B. Laktineh, M. Lethuillier, L. Mirabito, A.L. Pequegnot, S. Perries, J.D. Ruiz Alvarez, D. Sabes, L. Sgandurra, V. Sordini, M. Vander Donckt, P. Verdier, S. Viret

Georgian Technical University, Tbilisi, Georgia

T. Toriashvili¹⁷

Tbilisi State University, Tbilisi, Georgia

Z. Tsamalaidze¹⁰

RWTH Aachen University, I. Physikalisches Institut, Aachen, Germany

C. Autermann, S. Beranek, M. Edelhoff, L. Feld, A. Heister, M.K. Kiesel, K. Klein, M. Lipinski, A. Ostapchuk, M. Preuten, F. Raupach, S. Schael, J.F. Schulte, T. Verlage, H. Weber, B. Wittmer, V. Zhukov⁶

RWTH Aachen University, III. Physikalisches Institut A, Aachen, Germany

M. Ata, M. Brodski, E. Dietz-Laursonn, D. Duchardt, M. Endres, M. Erdmann, S. Erdweg, T. Esch, R. Fischer, A. Güth, T. Hebbeker, C. Heidemann, K. Hoepfner, D. Klingebiel, S. Knutzen, P. Kreuzer, M. Merschmeyer, A. Meyer, P. Millet, M. Olschewski, K. Padeken, P. Papacz, T. Pook, M. Radziej, H. Reithler, M. Rieger, F. Scheuch, L. Sonnenschein, D. Teysier, S. Thüer

RWTH Aachen University, III. Physikalisches Institut B, Aachen, Germany

V. Cherepanov, Y. Erdogan, G. Flügge, H. Geenen, M. Geisler, F. Hoehle, B. Kargoll, T. Kress, Y. Kuessel, A. Künsken, J. Lingemann², A. Nehr Korn, A. Nowack, I.M. Nugent, C. Pistone, O. Pooth, A. Stahl

Deutsches Elektronen-Synchrotron, Hamburg, Germany

M. Aldaya Martin, I. Asin, N. Bartosik, O. Behnke, U. Behrens, A.J. Bell, K. Borras, A. Burgmeier, A. Cakir, L. Calligaris, A. Campbell, S. Choudhury, F. Costanza, C. Diez Pardos, G. Dolinska, S. Dooling, T. Dorland, G. Eckerlin, D. Eckstein, T. Eichhorn, G. Flucke, E. Gallo¹⁸, J. Garay Garcia, A. Geiser, A. Gizhko, P. Gunnellini, J. Hauk, M. Hempel¹⁹, H. Jung,

A. Kalogeropoulos, O. Karacheban¹⁹, M. Kasemann, P. Katsas, J. Kieseler, C. Kleinwort, I. Korol, W. Lange, J. Leonard, K. Lipka, A. Lobanov, W. Lohmann¹⁹, R. Mankel, I. Marfin¹⁹, I.-A. Melzer-Pellmann, A.B. Meyer, G. Mittag, J. Mnich, A. Mussgiller, S. Naumann-Emme, A. Nayak, E. Ntomari, H. Perrey, D. Pitzl, R. Placakyte, A. Raspereza, B. Roland, M.Ö. Sahin, P. Saxena, T. Schoerner-Sadenius, M. Schröder, C. Seitz, S. Spannagel, K.D. Trippkewitz, R. Walsh, C. Wissing

University of Hamburg, Hamburg, Germany

V. Blobel, M. Centis Vignali, A.R. Draeger, J. Erfle, E. Garutti, K. Goebel, D. Gonzalez, M. Görner, J. Haller, M. Hoffmann, R.S. Höing, A. Junkes, R. Klanner, R. Kogler, T. Lapsien, T. Lenz, I. Marchesini, D. Marconi, M. Meyer, D. Nowatschin, J. Ott, F. Pantaleo², T. Peiffer, A. Perieanu, N. Pietsch, J. Poehlsen, D. Rathjens, C. Sander, H. Schettler, P. Schleper, E. Schlieckau, A. Schmidt, J. Schwandt, M. Seidel, V. Sola, H. Stadie, G. Steinbrück, H. Tholen, D. Troendle, E. Usai, L. Vanelderden, A. Vanhoefer, B. Vormwald

Institut für Experimentelle Kernphysik, Karlsruhe, Germany

M. Akbiyik, C. Barth, C. Baus, J. Berger, C. Böser, E. Butz, T. Chwalek, F. Colombo, W. De Boer, A. Descroix, A. Dierlamm, S. Fink, F. Frensch, M. Giffels, A. Gilbert, F. Hartmann², S.M. Heindl, U. Husemann, I. Katkov⁶, A. Kornmayer², P. Lobelle Pardo, B. Maier, H. Mildner, M.U. Mozer, T. Müller, Th. Müller, M. Plagge, G. Quast, K. Rabbertz, S. Röcker, F. Roscher, H.J. Simonis, F.M. Stober, R. Ulrich, J. Wagner-Kuhr, S. Wayand, M. Weber, T. Weiler, C. Wöhrmann, R. Wolf

Institute of Nuclear and Particle Physics (INPP), NCSR Demokritos, Aghia Paraskevi, Greece

G. Anagnostou, G. Daskalakis, T. Gerasis, V.A. Giakoumopoulou, A. Kyriakis, D. Loukas, A. Psallidas, I. Topsis-Giotis

University of Athens, Athens, Greece

A. Agapitos, S. Kesisoglou, A. Panagiotou, N. Saoulidou, E. Tziaferi

University of Ioánnina, Ioánnina, Greece

I. Evangelou, G. Flouris, C. Foudas, P. Kokkas, N. Loukas, N. Manthos, I. Papadopoulos, E. Paradas, J. Strologas

Wigner Research Centre for Physics, Budapest, Hungary

G. Bencze, C. Hajdu, A. Hazi, P. Hidas, D. Horvath²⁰, F. Sikler, V. Veszpremi, G. Vesztergombi²¹, A.J. Zsigmond

Institute of Nuclear Research ATOMKI, Debrecen, Hungary

N. Beni, S. Czellar, J. Karancsi²², J. Molnar, Z. Szillasi

University of Debrecen, Debrecen, Hungary

M. Bartók²³, A. Makovec, P. Raics, Z.L. Trocsanyi, B. Ujvari

National Institute of Science Education and Research, Bhubaneswar, India

P. Mal, K. Mandal, N. Sahoo, S.K. Swain

Panjab University, Chandigarh, India

S. Bansal, S.B. Beri, V. Bhatnagar, R. Chawla, R. Gupta, U. Bhawandeep, A.K. Kalsi, A. Kaur, M. Kaur, R. Kumar, A. Mehta, M. Mittal, J.B. Singh, G. Walia

University of Delhi, Delhi, India

Ashok Kumar, A. Bhardwaj, B.C. Choudhary, R.B. Garg, A. Kumar, S. Malhotra, M. Naimuddin, N. Nishu, K. Ranjan, R. Sharma, V. Sharma

Saha Institute of Nuclear Physics, Kolkata, India

S. Banerjee, S. Bhattacharya, K. Chatterjee, S. Dey, S. Dutta, Sa. Jain, N. Majumdar, A. Modak, K. Mondal, S. Mukherjee, S. Mukhopadhyay, A. Roy, D. Roy, S. Roy Chowdhury, S. Sarkar, M. Sharan

Bhabha Atomic Research Centre, Mumbai, India

A. Abdulsalam, R. Chudasama, D. Dutta, V. Jha, V. Kumar, A.K. Mohanty², L.M. Pant, P. Shukla, A. Topkar

Tata Institute of Fundamental Research, Mumbai, India

T. Aziz, S. Banerjee, S. Bhowmik²⁴, R.M. Chatterjee, R.K. Dewanjee, S. Dugad, S. Ganguly, S. Ghosh, M. Guchait, A. Gurtu²⁵, G. Kole, S. Kumar, B. Mahakud, M. Maity²⁴, G. Majumder, K. Mazumdar, S. Mitra, G.B. Mohanty, B. Parida, T. Sarkar²⁴, K. Sudhakar, N. Sur, B. Sutar, N. Wickramage²⁶

Indian Institute of Science Education and Research (IISER), Pune, India

S. Chauhan, S. Dube, S. Sharma

Institute for Research in Fundamental Sciences (IPM), Tehran, Iran

H. Bakhshiansohi, H. Behnamian, S.M. Etesami²⁷, A. Fahim²⁸, R. Goldouzian, M. Khakzad, M. Mohammadi Najafabadi, M. Naseri, S. Paktinat Mehdiabadi, F. Rezaei Hosseinabadi, B. Safarzadeh²⁹, M. Zeinali

University College Dublin, Dublin, Ireland

M. Felcini, M. Grunewald

INFN Sezione di Bari ^a, Università di Bari ^b, Politecnico di Bari ^c, Bari, Italy

M. Abbrescia^{a,b}, C. Calabria^{a,b}, C. Caputo^{a,b}, A. Colaleo^a, D. Creanza^{a,c}, L. Cristella^{a,b}, N. De Filippis^{a,c}, M. De Palma^{a,b}, L. Fiore^a, G. Iaselli^{a,c}, G. Maggi^{a,c}, M. Maggi^a, G. Miniello^{a,b}, S. My^{a,c}, S. Nuzzo^{a,b}, A. Pompili^{a,b}, G. Pugliese^{a,c}, R. Radogna^{a,b}, A. Ranieri^a, G. Selvaggi^{a,b}, L. Silvestris^{a,2}, R. Venditti^{a,b}, P. Verwilligen^a

INFN Sezione di Bologna ^a, Università di Bologna ^b, Bologna, Italy

G. Abbiendi^a, C. Battilana², A.C. Benvenuti^a, D. Bonacorsi^{a,b}, S. Braibant-Giacomelli^{a,b}, L. Brigliadori^{a,b}, R. Campanini^{a,b}, P. Capiluppi^{a,b}, A. Castro^{a,b}, F.R. Cavallo^a, S.S. Chhibra^{a,b}, G. Codispoti^{a,b}, M. Cuffiani^{a,b}, G.M. Dallavalle^a, F. Fabbri^a, A. Fanfani^{a,b}, D. Fasanella^{a,b}, P. Giacomelli^a, C. Grandi^a, L. Guiducci^{a,b}, S. Marcellini^a, G. Masetti^a, A. Montanari^a, F.L. Navarria^{a,b}, A. Perrotta^a, A.M. Rossi^{a,b}, T. Rovelli^{a,b}, G.P. Siroli^{a,b}, N. Tosi^{a,b}, R. Travaglini^{a,b}

INFN Sezione di Catania ^a, Università di Catania ^b, Catania, Italy

G. Cappello^a, M. Chiorboli^{a,b}, S. Costa^{a,b}, F. Giordano^{a,b}, R. Potenza^{a,b}, A. Tricomi^{a,b}, C. Tuve^{a,b}

INFN Sezione di Firenze ^a, Università di Firenze ^b, Firenze, Italy

G. Barbagli^a, V. Ciulli^{a,b}, C. Civinini^a, R. D'Alessandro^{a,b}, E. Focardi^{a,b}, S. Gonzi^{a,b}, V. Gori^{a,b}, P. Lenzi^{a,b}, M. Meschini^a, S. Paoletti^a, G. Sguazzoni^a, A. Tropiano^{a,b}, L. Viliani^{a,b}

INFN Laboratori Nazionali di Frascati, Frascati, Italy

L. Benussi, S. Bianco, F. Fabbri, D. Piccolo, F. Primavera

INFN Sezione di Genova ^a, Università di Genova ^b, Genova, Italy

V. Calvelli^{a,b}, F. Ferro^a, M. Lo Vetere^{a,b}, M.R. Monge^{a,b}, E. Robutti^a, S. Tosi^{a,b}

INFN Sezione di Milano-Bicocca ^a, Università di Milano-Bicocca ^b, Milano, Italy

L. Brianza, M.E. Dinardo^{a,b}, P. Dini^a, S. Fiorendi^{a,b}, S. Gennai^a, R. Gerosa^{a,b}, A. Ghezzi^{a,b}

P. Govoni^{a,b}, S. Malvezzi^a, R.A. Manzoni^{a,b}, B. Marzocchi^{a,b,2}, D. Menasce^a, L. Moroni^a, M. Paganoni^{a,b}, S. Ragazzi^{a,b}, N. Redaelli^a, T. Tabarelli de Fatis^{a,b}

INFN Sezione di Napoli^a, Università di Napoli 'Federico II'^b, Napoli, Italy, Università della Basilicata^c, Potenza, Italy, Università G. Marconi^d, Roma, Italy

S. Buontempo^a, N. Cavallo^{a,c}, S. Di Guida^{a,d,2}, M. Esposito^{a,b}, F. Fabozzi^{a,c}, A.O.M. Iorio^{a,b}, G. Lanza^a, L. Lista^a, S. Meola^{a,d,2}, M. Merola^a, P. Paolucci^{a,2}, C. Sciacca^{a,b}, F. Thyssen

INFN Sezione di Padova^a, Università di Padova^b, Padova, Italy, Università di Trento^c, Trento, Italy

P. Azzi^{a,2}, N. Bacchetta^a, L. Benato^{a,b}, D. Bisello^{a,b}, A. Boletti^{a,b}, A. Branca^{a,b}, R. Carlin^{a,b}, P. Checchia^a, M. Dall'Osso^{a,b,2}, T. Dorigo^a, U. Dosselli^a, F. Gasparini^{a,b}, U. Gasparini^{a,b}, A. Gozzelino^a, S. Lacaprara^a, M. Margoni^{a,b}, A.T. Meneguzzo^{a,b}, F. Montecassiano^a, M. Passaseo^a, J. Pazzini^{a,b}, N. Pozzobon^{a,b}, P. Ronchese^{a,b}, F. Simonetto^{a,b}, E. Torassa^a, M. Tosi^{a,b}, M. Zanetti, P. Zotto^{a,b}, A. Zucchetta^{a,b,2}, G. Zumerle^{a,b}

INFN Sezione di Pavia^a, Università di Pavia^b, Pavia, Italy

A. Braghieri^a, A. Magnani^a, P. Montagna^{a,b}, S.P. Ratti^{a,b}, V. Re^a, C. Riccardi^{a,b}, P. Salvini^a, I. Vai^a, P. Vitulo^{a,b}

INFN Sezione di Perugia^a, Università di Perugia^b, Perugia, Italy

L. Alunni Solestizi^{a,b}, M. Biasini^{a,b}, G.M. Bilei^a, D. Ciangottini^{a,b,2}, L. Fanò^{a,b}, P. Lariccia^{a,b}, G. Mantovani^{a,b}, M. Menichelli^a, A. Saha^a, A. Santocchia^{a,b}, A. Spiezia^{a,b}

INFN Sezione di Pisa^a, Università di Pisa^b, Scuola Normale Superiore di Pisa^c, Pisa, Italy

K. Androsov^{a,30}, P. Azzurri^a, G. Bagliesi^a, J. Bernardini^a, T. Boccali^a, G. Broccolo^{a,c}, R. Castaldi^a, M.A. Ciocci^{a,30}, R. Dell'Orso^a, S. Donato^{a,c,2}, G. Fedi, L. Foà^{a,c†}, A. Giassi^a, M.T. Grippo^{a,30}, F. Ligabue^{a,c}, T. Lomtadze^a, L. Martini^{a,b}, A. Messineo^{a,b}, F. Palla^a, A. Rizzi^{a,b}, A. Savoy-Navarro^{a,31}, A.T. Serban^a, P. Spagnolo^a, P. Squillacioti^{a,30}, R. Tenchini^a, G. Tonelli^{a,b}, A. Venturi^a, P.G. Verdini^a

INFN Sezione di Roma^a, Università di Roma^b, Roma, Italy

L. Barone^{a,b}, F. Cavallari^a, G. D'imperio^{a,b,2}, D. Del Re^{a,b}, M. Diemoz^a, S. Gelli^{a,b}, C. Jorda^a, E. Longo^{a,b}, F. Margaroli^{a,b}, P. Meridiani^a, G. Organtini^{a,b}, R. Paramatti^a, F. Preiato^{a,b}, S. Rahatlou^{a,b}, C. Rovelli^a, F. Santanastasio^{a,b}, P. Traczyk^{a,b,2}

INFN Sezione di Torino^a, Università di Torino^b, Torino, Italy, Università del Piemonte Orientale^c, Novara, Italy

N. Amapane^{a,b}, R. Arcidiacono^{a,c,2}, S. Argiro^{a,b}, M. Arneodo^{a,c}, R. Bellan^{a,b}, C. Biino^a, N. Cartiglia^a, M. Costa^{a,b}, R. Covarelli^{a,b}, A. Degano^{a,b}, N. Demaria^a, L. Finco^{a,b,2}, B. Kiani^{a,b}, C. Mariotti^a, S. Maselli^a, E. Migliore^{a,b}, V. Monaco^{a,b}, E. Monteil^{a,b}, M. Musich^a, M.M. Obertino^{a,b}, L. Pacher^{a,b}, N. Pastrone^a, M. Pelliccioni^a, G.L. Pinna Angioni^{a,b}, F. Ravera^{a,b}, A. Romero^{a,b}, M. Ruspa^{a,c}, R. Sacchi^{a,b}, A. Solano^{a,b}, A. Staiano^a, U. Tamponi^a

INFN Sezione di Trieste^a, Università di Trieste^b, Trieste, Italy

S. Belforte^a, V. Candelise^{a,b,2}, M. Casarsa^a, F. Cossutti^a, G. Della Ricca^{a,b}, B. Gobbo^a, C. La Licata^{a,b}, M. Marone^{a,b}, A. Schizzi^{a,b}, A. Zanetti^a

Kangwon National University, Chunchon, Korea

A. Kropivnitskaya, S.K. Nam

Kyungpook National University, Daegu, Korea

D.H. Kim, G.N. Kim, M.S. Kim, D.J. Kong, S. Lee, Y.D. Oh, A. Sakharov, D.C. Son

Chonbuk National University, Jeonju, Korea

J.A. Brochero Cifuentes, H. Kim, T.J. Kim, M.S. Ryu

Chonnam National University, Institute for Universe and Elementary Particles, Kwangju, Korea

S. Song

Korea University, Seoul, Korea

S. Choi, Y. Go, D. Gyun, B. Hong, M. Jo, H. Kim, Y. Kim, B. Lee, K. Lee, K.S. Lee, S. Lee, S.K. Park, Y. Roh

Seoul National University, Seoul, Korea

H.D. Yoo

University of Seoul, Seoul, Korea

M. Choi, H. Kim, J.H. Kim, J.S.H. Lee, I.C. Park, G. Ryu

Sungkyunkwan University, Suwon, Korea

Y. Choi, Y.K. Choi, J. Goh, D. Kim, E. Kwon, J. Lee, I. Yu

Vilnius University, Vilnius, Lithuania

A. Juodagalvis, J. Vaitkus

National Centre for Particle Physics, Universiti Malaya, Kuala Lumpur, Malaysia

I. Ahmed, Z.A. Ibrahim, J.R. Komaragiri, M.A.B. Md Ali³², F. Mohamad Idris³³, W.A.T. Wan Abdullah, M.N. Yusli

Centro de Investigacion y de Estudios Avanzados del IPN, Mexico City, Mexico

E. Casimiro Linares, H. Castilla-Valdez, E. De La Cruz-Burelo, I. Heredia-de La Cruz³⁴, A. Hernandez-Almada, R. Lopez-Fernandez, A. Sanchez-Hernandez

Universidad Iberoamericana, Mexico City, Mexico

S. Carrillo Moreno, F. Vazquez Valencia

Benemerita Universidad Autonoma de Puebla, Puebla, Mexico

I. Pedraza, H.A. Salazar Ibarguen

Universidad Autónoma de San Luis Potosí, San Luis Potosí, Mexico

A. Morelos Pineda

University of Auckland, Auckland, New Zealand

D. Krofcheck

University of Canterbury, Christchurch, New Zealand

P.H. Butler

National Centre for Physics, Quaid-I-Azam University, Islamabad, Pakistan

A. Ahmad, M. Ahmad, Q. Hassan, H.R. Hoorani, W.A. Khan, T. Khurshid, M. Shoaib

National Centre for Nuclear Research, Swierk, Poland

H. Bialkowska, M. Bluj, B. Boimska, T. Frueboes, M. Górski, M. Kazana, K. Nawrocki, K. Romanowska-Rybinska, M. Szleper, P. Zalewski

Institute of Experimental Physics, Faculty of Physics, University of Warsaw, Warsaw, Poland

G. Brona, K. Bunkowski, A. Byszuk³⁵, K. Doroba, A. Kalinowski, M. Konecki, J. Krolikowski, M. Misiura, M. Olszewski, M. Walczak

Laboratório de Instrumentação e Física Experimental de Partículas, Lisboa, Portugal

P. Bargassa, C. Beirão Da Cruz E Silva, A. Di Francesco, P. Faccioli, P.G. Ferreira Parracho, M. Gallinaro, N. Leonardo, L. Lloret Iglesias, F. Nguyen, J. Rodrigues Antunes, J. Seixas, O. Toldaiev, D. Vadrucio, J. Varela, P. Vischia

Joint Institute for Nuclear Research, Dubna, Russia

S. Afanasiev, P. Bunin, M. Gavrilenko, I. Golutvin, I. Gorbunov, A. Kamenev, V. Karjavin, V. Konoplyanikov, A. Lanev, A. Malakhov, V. Matveev³⁶, P. Moiseenz, V. Palichik, V. Perelygin, S. Shmatov, S. Shulha, N. Skatchkov, V. Smirnov, A. Zarubin

Petersburg Nuclear Physics Institute, Gatchina (St. Petersburg), Russia

V. Golovtsov, Y. Ivanov, V. Kim³⁷, E. Kuznetsova, P. Levchenko, V. Murzin, V. Oreshkin, I. Smirnov, V. Sulimov, L. Uvarov, S. Vavilov, A. Vorobyev

Institute for Nuclear Research, Moscow, Russia

Yu. Andreev, A. Dermenev, S. Gninenko, N. Golubev, A. Karneyeu, M. Kirsanov, N. Krasnikov, A. Pashenkov, D. Tlisov, A. Toropin

Institute for Theoretical and Experimental Physics, Moscow, Russia

V. Epshteyn, V. Gavrillov, N. Lychkovskaya, V. Popov, I. Pozdnyakov, G. Safronov, A. Spiridonov, E. Vlasov, A. Zhokin

National Research Nuclear University 'Moscow Engineering Physics Institute' (MEPhI), Moscow, Russia

A. Bylinkin

P.N. Lebedev Physical Institute, Moscow, Russia

V. Andreev, M. Azarkin³⁸, I. Dremin³⁸, M. Kirakosyan, A. Leonidov³⁸, G. Mesyats, S.V. Rusakov, A. Vinogradov

Skobeltsyn Institute of Nuclear Physics, Lomonosov Moscow State University, Moscow, Russia

A. Baskakov, A. Belyaev, E. Boos, V. Bunichev, M. Dubinin³⁹, L. Dudko, A. Gribushin, V. Klyukhin, O. Kodolova, I. Lokhtin, I. Myagkov, S. Obraztsov, S. Petrushanko, V. Savrin, A. Snigirev

State Research Center of Russian Federation, Institute for High Energy Physics, Protvino, Russia

I. Azhgirey, I. Bayshev, S. Bitioukov, V. Kachanov, A. Kalinin, D. Konstantinov, V. Krychkin, V. Petrov, R. Ryutin, A. Sobol, L. Tourtchanovitch, S. Troshin, N. Tyurin, A. Uzunian, A. Volkov

University of Belgrade, Faculty of Physics and Vinca Institute of Nuclear Sciences, Belgrade, Serbia

P. Adzic⁴⁰, M. Ekmedzic, J. Milosevic, V. Rekovic

Centro de Investigaciones Energéticas Medioambientales y Tecnológicas (CIEMAT), Madrid, Spain

J. Alcaraz Maestre, E. Calvo, M. Cerrada, M. Chamizo Llatas, N. Colino, B. De La Cruz, A. Delgado Peris, D. Domínguez Vázquez, A. Escalante Del Valle, C. Fernandez Bedoya, J.P. Fernández Ramos, J. Flix, M.C. Fouz, P. Garcia-Abia, O. Gonzalez Lopez, S. Goy Lopez, J.M. Hernandez, M.I. Josa, E. Navarro De Martino, A. Pérez-Calero Yzquierdo, J. Puerta Pelayo, A. Quintario Olmeda, I. Redondo, L. Romero, M.S. Soares

Universidad Autónoma de Madrid, Madrid, Spain

C. Albajar, J.F. de Trocóniz, M. Missiroli, D. Moran

Universidad de Oviedo, Oviedo, Spain

J. Cuevas, J. Fernandez Menendez, S. Folgueras, I. Gonzalez Caballero, E. Palencia Cortezon, J.M. Vizan Garcia

Instituto de Física de Cantabria (IFCA), CSIC-Universidad de Cantabria, Santander, Spain

I.J. Cabrillo, A. Calderon, J.R. Castiñeiras De Saa, P. De Castro Manzano, J. Duarte Campderros, M. Fernandez, J. Garcia-Ferrero, G. Gomez, A. Lopez Virto, J. Marco, R. Marco, C. Martinez Rivero, F. Matorras, F.J. Munoz Sanchez, J. Piedra Gomez, T. Rodrigo, A.Y. Rodríguez-Marrero, A. Ruiz-Jimeno, L. Scodellaro, I. Vila, R. Vilar Cortabitarte

CERN, European Organization for Nuclear Research, Geneva, Switzerland

D. Abbaneo, E. Auffray, G. Auzinger, M. Bachtis, P. Baillon, A.H. Ball, D. Barney, A. Benaglia, J. Bendavid, L. Benhabib, J.F. Benitez, G.M. Berruti, P. Bloch, A. Bocci, A. Bonato, C. Botta, H. Breuker, T. Camporesi, G. Cerminara, S. Colafranceschi⁴¹, M. D'Alfonso, D. d'Enterria, A. Dabrowski, V. Daponte, A. David, M. De Gruttola, F. De Guio, A. De Roeck, S. De Visscher, E. Di Marco, M. Dobson, M. Dordevic, B. Dorney, T. du Pree, M. Dünser, N. Dupont, A. Elliott-Peisert, G. Franzoni, W. Funk, D. Gigi, K. Gill, D. Giordano, M. Girone, F. Glege, R. Guida, S. Gundacker, M. Guthoff, J. Hammer, P. Harris, J. Hegeman, V. Innocente, P. Janot, H. Kirschenmann, M.J. Kortelainen, K. Kousouris, K. Krajczar, P. Lecoq, C. Lourenço, M.T. Lucchini, N. Magini, L. Malgeri, M. Mannelli, A. Martelli, L. Masetti, F. Meijers, S. Mersi, E. Meschi, F. Moortgat, S. Morovic, M. Mulders, M.V. Nemallapudi, H. Neugebauer, S. Orfanelli⁴², L. Orsini, L. Pape, E. Perez, M. Peruzzi, A. Petrilli, G. Petrucciani, A. Pfeiffer, D. Piparo, A. Racz, G. Rolandi⁴³, M. Rovere, M. Ruan, H. Sakulin, C. Schäfer, C. Schwick, A. Sharma, P. Silva, M. Simon, P. Sphicas⁴⁴, D. Spiga, J. Steggemann, B. Stieger, M. Stoye, Y. Takahashi, D. Treille, A. Triossi, A. Tsirou, G.I. Veres²¹, N. Wardle, H.K. Wöhri, A. Zagozdzińska³⁵, W.D. Zeuner

Paul Scherrer Institut, Villigen, Switzerland

W. Bertl, K. Deiters, W. Erdmann, R. Horisberger, Q. Ingram, H.C. Kaestli, D. Kotlinski, U. Langenegger, D. Renker, T. Rohe

Institute for Particle Physics, ETH Zurich, Zurich, Switzerland

F. Bachmair, L. Bäni, L. Bianchini, M.A. Buchmann, B. Casal, G. Dissertori, M. Dittmar, M. Donegà, P. Eller, C. Grab, C. Heidegger, D. Hits, J. Hoss, G. Kasieczka, W. Lustermann, B. Mangano, M. Marionneau, P. Martinez Ruiz del Arbol, M. Masciovecchio, D. Meister, F. Micheli, P. Musella, F. Nessi-Tedaldi, F. Pandolfi, J. Pata, F. Pauss, L. Perrozzi, M. Quitnat, M. Rossini, A. Starodumov⁴⁵, M. Takahashi, V.R. Tavolaro, K. Theofilatos, R. Wallny

Universität Zürich, Zurich, Switzerland

T.K. Aarrestad, C. AMSler⁴⁶, L. Caminada, M.F. Canelli, V. Chiochia, A. De Cosa, C. Galloni, A. Hinzmann, T. Hreus, B. Kilminster, C. Lange, J. Ngadiuba, D. Pinna, P. Robmann, F.J. Ronga, D. Salerno, Y. Yang

National Central University, Chung-Li, Taiwan

M. Cardaci, K.H. Chen, T.H. Doan, Sh. Jain, R. Khurana, M. Konyushikhin, C.M. Kuo, W. Lin, Y.J. Lu, S.S. Yu

National Taiwan University (NTU), Taipei, Taiwan

Arun Kumar, R. Bartek, P. Chang, Y.H. Chang, Y.W. Chang, Y. Chao, K.F. Chen, P.H. Chen, C. Dietz, F. Fiori, U. Grundler, W.-S. Hou, Y. Hsiung, Y.F. Liu, R.-S. Lu, M. Miñano Moya, E. Petrakou, J.F. Tsai, Y.M. Tzeng

Chulalongkorn University, Faculty of Science, Department of Physics, Bangkok, Thailand

B. Asavapibhop, K. Kovitanggoon, G. Singh, N. Srimanobhas, N. Suwonjandee

Cukurova University, Adana, Turkey

A. Adiguzel, M.N. Bakirci⁴⁷, Z.S. Demiroglu, C. Dozen, I. Dumanoglu, E. Eskut, S. Girgis, G. Gokbulut, Y. Guler, E. Gurpinar, I. Hos, E.E. Kangal⁴⁸, G. Onengut⁴⁹, K. Ozdemir⁵⁰, A. Polatoz, D. Sunar Cerci⁵¹, B. Tali⁵¹, M. Vergili, C. Zorbilmez

Middle East Technical University, Physics Department, Ankara, Turkey

I.V. Akin, B. Bilin, S. Bilmis, B. Isildak⁵², G. Karapinar⁵³, M. Yalvac, M. Zeyrek

Bogazici University, Istanbul, Turkey

E.A. Albayrak⁵⁴, E. Gülmez, M. Kaya⁵⁵, O. Kaya⁵⁶, T. Yetkin⁵⁷

Istanbul Technical University, Istanbul, Turkey

K. Cankocak, S. Sen⁵⁸, F.I. Vardarli

Institute for Scintillation Materials of National Academy of Science of Ukraine, Kharkov, Ukraine

B. Grynyov

National Scientific Center, Kharkov Institute of Physics and Technology, Kharkov, Ukraine

L. Levchuk, P. Sorokin

University of Bristol, Bristol, United Kingdom

R. Aggleton, F. Ball, L. Beck, J.J. Brooke, E. Clement, D. Cussans, H. Flacher, J. Goldstein, M. Grimes, G.P. Heath, H.F. Heath, J. Jacob, L. Kreczko, C. Lucas, Z. Meng, D.M. Newbold⁵⁹, S. Paramesvaran, A. Poll, T. Sakuma, S. Seif El Nasr-storey, S. Senkin, D. Smith, V.J. Smith

Rutherford Appleton Laboratory, Didcot, United Kingdom

K.W. Bell, A. Belyaev⁶⁰, C. Brew, R.M. Brown, D. Cieri, D.J.A. Cockerill, J.A. Coughlan, K. Harder, S. Harper, E. Olaiya, D. Petyt, C.H. Shepherd-Themistocleous, A. Thea, L. Thomas, I.R. Tomalin, T. Williams, W.J. Womersley, S.D. Worm

Imperial College, London, United Kingdom

M. Baber, R. Bainbridge, O. Buchmuller, A. Bundock, D. Burton, S. Casasso, M. Citron, D. Colling, L. Corpe, N. Cripps, P. Dauncey, G. Davies, A. De Wit, M. Della Negra, P. Dunne, A. Elwood, W. Ferguson, J. Fulcher, D. Futyan, G. Hall, G. Iles, M. Kenzie, R. Lane, R. Lucas⁵⁹, L. Lyons, A.-M. Magnan, S. Malik, J. Nash, A. Nikitenko⁴⁵, J. Pela, M. Pesaresi, K. Petridis, D.M. Raymond, A. Richards, A. Rose, C. Seez, A. Tapper, K. Uchida, M. Vazquez Acosta⁶¹, T. Virdee, S.C. Zenz

Brunel University, Uxbridge, United Kingdom

J.E. Cole, P.R. Hobson, A. Khan, P. Kyberd, D. Leggat, D. Leslie, I.D. Reid, P. Symonds, L. Teodorescu, M. Turner

Baylor University, Waco, USA

A. Borzou, K. Call, J. Dittmann, K. Hatakeyama, A. Kasmi, H. Liu, N. Pastika

The University of Alabama, Tuscaloosa, USA

O. Charaf, S.I. Cooper, C. Henderson, P. Rumerio

Boston University, Boston, USA

A. Avetisyan, T. Bose, C. Fantasia, D. Gastler, P. Lawson, D. Rankin, C. Richardson, J. Rohlf, J. St. John, L. Sulak, D. Zou

Brown University, Providence, USA

J. Alimena, E. Berry, S. Bhattacharya, D. Cutts, N. Dhingra, A. Ferapontov, A. Garabedian, J. Hakala, U. Heintz, E. Laird, G. Landsberg, Z. Mao, M. Narain, S. Piperov, S. Sagir, T. Sinthuprasith, R. Syarif

University of California, Davis, Davis, USA

R. Breedon, G. Breto, M. Calderon De La Barca Sanchez, S. Chauhan, M. Chertok, J. Conway, R. Conway, P.T. Cox, R. Erbacher, M. Gardner, W. Ko, R. Lander, M. Mulhearn, D. Pellett, J. Pilot, F. Ricci-Tam, S. Shalhout, J. Smith, M. Squires, D. Stolp, M. Tripathi, S. Wilbur, R. Yohay

University of California, Los Angeles, USA

R. Cousins, P. Everaerts, C. Farrell, J. Hauser, M. Ignatenko, D. Saltzberg, E. Takasugi, V. Valuev, M. Weber

University of California, Riverside, Riverside, USA

K. Burt, R. Clare, J. Ellison, J.W. Gary, G. Hanson, J. Heilman, M. Ivova PANEVA, P. Jandir, E. Kennedy, F. Lacroix, O.R. Long, A. Luthra, M. Malberti, M. Olmedo Negrete, A. Shrinivas, H. Wei, S. Wimpenny, B. R. Yates

University of California, San Diego, La Jolla, USA

J.G. Branson, G.B. Cerati, S. Cittolin, R.T. D'Agnolo, A. Holzner, R. Kelley, D. Klein, J. Letts, I. Macneill, D. Olivito, S. Padhi, M. Pieri, M. Sani, V. Sharma, S. Simon, M. Tadel, A. Vartak, S. Wasserbaech⁶², C. Welke, F. Würthwein, A. Yagil, G. Zevi Della Porta

University of California, Santa Barbara, Santa Barbara, USA

D. Barge, J. Bradmiller-Feld, C. Campagnari, A. Dishaw, V. Dutta, K. Flowers, M. Franco Sevilla, P. Geffert, C. George, F. Golf, L. Gouskos, J. Gran, J. Incandela, C. Justus, N. Mccoll, S.D. Mullin, J. Richman, D. Stuart, I. Suarez, W. To, C. West, J. Yoo

California Institute of Technology, Pasadena, USA

D. Anderson, A. Apresyan, A. Bornheim, J. Bunn, Y. Chen, J. Duarte, A. Mott, H.B. Newman, C. Pena, M. Pierini, M. Spiropulu, J.R. Vlimant, S. Xie, R.Y. Zhu

Carnegie Mellon University, Pittsburgh, USA

M.B. Andrews, V. Azzolini, A. Calamba, B. Carlson, T. Ferguson, M. Paulini, J. Russ, M. Sun, H. Vogel, I. Vorobiev

University of Colorado Boulder, Boulder, USA

J.P. Cumalat, W.T. Ford, A. Gaz, F. Jensen, A. Johnson, M. Krohn, T. Mulholland, U. Nauenberg, K. Stenson, S.R. Wagner

Cornell University, Ithaca, USA

J. Alexander, A. Chatterjee, J. Chaves, J. Chu, S. Dittmer, N. Eggert, N. Mirman, G. Nicolas Kaufman, J.R. Patterson, A. Rinkevicius, A. Ryd, L. Skinnari, L. Soffi, W. Sun, S.M. Tan, W.D. Teo, J. Thom, J. Thompson, J. Tucker, Y. Weng, P. Wittich

Fermi National Accelerator Laboratory, Batavia, USA

S. Abdullin, M. Albrow, J. Anderson, G. Apollinari, L.A.T. Bauerdick, A. Beretvas, J. Berryhill, P.C. Bhat, G. Bolla, K. Burkett, J.N. Butler, H.W.K. Cheung, F. Chlebana, S. Cihangir, V.D. Elvira, I. Fisk, J. Freeman, E. Gottschalk, L. Gray, D. Green, S. Grünendahl, O. Gutsche, J. Hanlon, D. Hare, R.M. Harris, J. Hirschauer, Z. Hu, S. Jindariani, M. Johnson, U. Joshi, A.W. Jung, B. Klima, B. Kreis, S. Kwan[†], S. Lammel, J. Linacre, D. Lincoln, R. Lipton, T. Liu, R. Lopes De Sá, J. Lykken, K. Maeshima, J.M. Marraffino, V.I. Martinez Outschoorn, S. Maruyama, D. Mason, P. McBride, P. Merkel, K. Mishra, S. Mrenna, S. Nahn, C. Newman-Holmes, V. O'Dell, K. Pedro,

O. Prokofyev, G. Rakness, E. Sexton-Kennedy, A. Soha, W.J. Spalding, L. Spiegel, L. Taylor, S. Tkaczyk, N.V. Tran, L. Uplegger, E.W. Vaandering, C. Vernieri, M. Verzocchi, R. Vidal, H.A. Weber, A. Whitbeck, F. Yang

University of Florida, Gainesville, USA

D. Acosta, P. Avery, P. Bortignon, D. Bourilkov, A. Carnes, M. Carver, D. Curry, S. Das, G.P. Di Giovanni, R.D. Field, I.K. Furic, J. Hugon, J. Konigsberg, A. Korytov, J.F. Low, P. Ma, K. Matchev, H. Mei, P. Milenovic⁶³, G. Mitselmakher, D. Rank, R. Rossin, L. Shchutska, M. Snowball, D. Sperka, N. Terentyev, J. Wang, S. Wang, J. Yelton

Florida International University, Miami, USA

S. Hewamanage, S. Linn, P. Markowitz, G. Martinez, J.L. Rodriguez

Florida State University, Tallahassee, USA

A. Ackert, J.R. Adams, T. Adams, A. Askew, J. Bochenek, B. Diamond, J. Haas, S. Hagopian, V. Hagopian, K.F. Johnson, A. Khatiwada, H. Prosper, V. Veeraraghavan, M. Weinberg

Florida Institute of Technology, Melbourne, USA

M.M. Baarmand, V. Bhopatkar, M. Hohlmann, H. Kalakhety, D. Noonan, T. Roy, F. Yumiceva

University of Illinois at Chicago (UIC), Chicago, USA

M.R. Adams, L. Apanasevich, D. Berry, R.R. Betts, I. Bucinskaite, R. Cavanaugh, O. Evdokimov, L. Gauthier, C.E. Gerber, D.J. Hofman, P. Kurt, C. O'Brien, I.D. Sandoval Gonzalez, C. Silkworth, P. Turner, N. Varelas, Z. Wu, M. Zakaria

The University of Iowa, Iowa City, USA

B. Bilki⁶⁴, W. Clarida, K. Dilsiz, S. Durgut, R.P. Gandrajula, M. Haytmyradov, V. Khristenko, J.-P. Merlo, H. Mermerkaya⁶⁵, A. Mestvirishvili, A. Moeller, J. Nachtman, H. Ogul, Y. Onel, F. Ozok⁵⁴, A. Penzo, C. Snyder, P. Tan, E. Tiras, J. Wetzel, K. Yi

Johns Hopkins University, Baltimore, USA

I. Anderson, B.A. Barnett, B. Blumenfeld, D. Fehling, L. Feng, A.V. Gritsan, P. Maksimovic, C. Martin, M. Osherson, M. Swartz, M. Xiao, Y. Xin, C. You

The University of Kansas, Lawrence, USA

P. Baringer, A. Bean, G. Benelli, C. Bruner, R.P. Kenny III, D. Majumder, M. Malek, M. Murray, S. Sanders, R. Stringer, Q. Wang

Kansas State University, Manhattan, USA

A. Ivanov, K. Kaadze, S. Khalil, M. Makouski, Y. Maravin, A. Mohammadi, L.K. Saini, N. Skhirtladze, S. Toda

Lawrence Livermore National Laboratory, Livermore, USA

D. Lange, F. Rebassoo, D. Wright

University of Maryland, College Park, USA

C. Anelli, A. Baden, O. Baron, A. Belloni, B. Calvert, S.C. Eno, C. Ferraioli, J.A. Gomez, N.J. Hadley, S. Jabeen, R.G. Kellogg, T. Kolberg, J. Kunkle, Y. Lu, A.C. Mignerey, Y.H. Shin, A. Skuja, M.B. Tonjes, S.C. Tonwar

Massachusetts Institute of Technology, Cambridge, USA

A. Apyan, R. Barbieri, A. Baty, K. Bierwagen, S. Brandt, W. Busza, I.A. Cali, Z. Demiragli, L. Di Matteo, G. Gomez Ceballos, M. Goncharov, D. Gulhan, Y. Iiyama, G.M. Innocenti, M. Klute, D. Kovalskyi, Y.S. Lai, Y.-J. Lee, A. Levin, P.D. Luckey, A.C. Marini, C. Mcginn, C. Mironov, X. Niu, C. Paus, D. Ralph, C. Roland, G. Roland, J. Salfeld-Nebgen, G.S.F. Stephens,

K. Sumorok, M. Varma, D. Velicanu, J. Veverka, J. Wang, T.W. Wang, B. Wyslouch, M. Yang, V. Zhukova

University of Minnesota, Minneapolis, USA

B. Dahmes, A. Evans, A. Finkel, A. Gude, P. Hansen, S. Kalafut, S.C. Kao, K. Klapoetke, Y. Kubota, Z. Lesko, J. Mans, S. Nourbakhsh, N. Ruckstuhl, R. Rusack, N. Tambe, J. Turkewitz

University of Mississippi, Oxford, USA

J.G. Acosta, S. Oliveros

University of Nebraska-Lincoln, Lincoln, USA

E. Avdeeva, K. Bloom, S. Bose, D.R. Claes, A. Dominguez, C. Fangmeier, R. Gonzalez Suarez, R. Kamalieddin, J. Keller, D. Knowlton, I. Kravchenko, J. Lazo-Flores, F. Meier, J. Monroy, F. Ratnikov, J.E. Siado, G.R. Snow

State University of New York at Buffalo, Buffalo, USA

M. Alyari, J. Dolen, J. George, A. Godshalk, C. Harrington, I. Iashvili, J. Kaisen, A. Kharchilava, A. Kumar, S. Rappoccio

Northeastern University, Boston, USA

G. Alverson, E. Barberis, D. Baumgartel, M. Chasco, A. Hortiangtham, A. Massironi, D.M. Morse, D. Nash, T. Orimoto, R. Teixeira De Lima, D. Trocino, R.-J. Wang, D. Wood, J. Zhang

Northwestern University, Evanston, USA

K.A. Hahn, A. Kubik, N. Mucia, N. Odell, B. Pollack, A. Pozdnyakov, M. Schmitt, S. Stoynev, K. Sung, M. Trovato, M. Velasco

University of Notre Dame, Notre Dame, USA

A. Brinkerhoff, N. Dev, M. Hildreth, C. Jessop, D.J. Karmgard, N. Kellams, K. Lannon, S. Lynch, N. Marinelli, F. Meng, C. Mueller, Y. Musienko³⁶, T. Pearson, M. Planer, A. Reinsvold, R. Ruchti, G. Smith, S. Taroni, N. Valls, M. Wayne, M. Wolf, A. Woodard

The Ohio State University, Columbus, USA

L. Antonelli, J. Brinson, B. Bylsma, L.S. Durkin, S. Flowers, A. Hart, C. Hill, R. Hughes, W. Ji, K. Kotov, T.Y. Ling, B. Liu, W. Luo, D. Puigh, M. Rodenburg, B.L. Winer, H.W. Wulsin

Princeton University, Princeton, USA

O. Driga, P. Elmer, J. Hardenbrook, P. Hebda, S.A. Koay, P. Lujan, D. Marlow, T. Medvedeva, M. Mooney, J. Olsen, C. Palmer, P. Piroué, X. Quan, H. Saka, D. Stickland, C. Tully, J.S. Werner, A. Zuranski

University of Puerto Rico, Mayaguez, USA

S. Malik

Purdue University, West Lafayette, USA

V.E. Barnes, D. Benedetti, D. Bortoletto, L. Gutay, M.K. Jha, M. Jones, K. Jung, M. Kress, D.H. Miller, N. Neumeister, B.C. Radburn-Smith, X. Shi, I. Shipsey, D. Silvers, J. Sun, A. Svyatkovskiy, F. Wang, W. Xie, L. Xu

Purdue University Calumet, Hammond, USA

N. Parashar, J. Stupak

Rice University, Houston, USA

A. Adair, B. Akgun, Z. Chen, K.M. Ecklund, F.J.M. Geurts, M. Guilbaud, W. Li, B. Michlin, M. Northup, B.P. Padley, R. Redjimi, J. Roberts, J. Rorie, Z. Tu, J. Zabel

University of Rochester, Rochester, USA

B. Betchart, A. Bodek, P. de Barbaro, R. Demina, Y. Eshaq, T. Ferbel, M. Galanti, A. Garcia-Bellido, J. Han, A. Harel, O. Hindrichs, A. Khukhunaishvili, G. Petrillo, M. Verzetti

The Rockefeller University, New York, USA

L. Demortier

Rutgers, The State University of New Jersey, Piscataway, USA

S. Arora, A. Barker, J.P. Chou, C. Contreras-Campana, E. Contreras-Campana, D. Duggan, D. Ferencek, Y. Gershtein, R. Gray, E. Halkiadakis, D. Hidas, E. Hughes, S. Kaplan, R. Kunnawalkam Elayavalli, A. Lath, K. Nash, S. Panwalkar, M. Park, S. Salur, S. Schnetzer, D. Sheffield, S. Somalwar, R. Stone, S. Thomas, P. Thomassen, M. Walker

University of Tennessee, Knoxville, USA

M. Foerster, G. Riley, K. Rose, S. Spanier, A. York

Texas A&M University, College Station, USA

O. Bouhali⁶⁶, A. Castaneda Hernandez⁶⁶, M. Dalchenko, M. De Mattia, A. Delgado, S. Dildick, R. Eusebi, W. Flanagan, J. Gilmore, T. Kamon⁶⁷, V. Krutelyov, R. Mueller, I. Osipenkov, Y. Pakhotin, R. Patel, A. Perloff, A. Rose, A. Safonov, A. Tatarinov, K.A. Ulmer²

Texas Tech University, Lubbock, USA

N. Akchurin, C. Cowden, J. Damgov, C. Dragoiu, P.R. Duerdo, J. Faulkner, S. Kunori, K. Lamichhane, S.W. Lee, T. Libeiro, S. Undleeb, I. Volobouev

Vanderbilt University, Nashville, USA

E. Appelt, A.G. Delannoy, S. Greene, A. Gurrola, R. Janjam, W. Johns, C. Maguire, Y. Mao, A. Melo, H. Ni, P. Sheldon, B. Snook, S. Tuo, J. Velkovska, Q. Xu

University of Virginia, Charlottesville, USA

M.W. Arenton, S. Boutle, B. Cox, B. Francis, J. Goodell, R. Hirosky, A. Ledovskoy, H. Li, C. Lin, C. Neu, Y. Wang, E. Wolfe, J. Wood, F. Xia

Wayne State University, Detroit, USA

C. Clarke, R. Harr, P.E. Karchin, C. Kottachchi Kankanamge Don, P. Lamichhane, J. Sturdy

University of Wisconsin, Madison, USA

D.A. Belknap, D. Carlsmith, M. Cepeda, S. Dasu, L. Dodd, S. Duric, E. Friis, B. Gomer, M. Grothe, R. Hall-Wilton, M. Herndon, A. Hervé, P. Klabbers, A. Lanaro, A. Levine, K. Long, R. Loveless, A. Mohapatra, I. Ojalvo, T. Perry, G.A. Pierro, G. Polese, T. Ruggles, T. Sarangi, A. Savin, A. Sharma, N. Smith, W.H. Smith, D. Taylor, N. Woods

†: Deceased

1: Also at Vienna University of Technology, Vienna, Austria

2: Also at CERN, European Organization for Nuclear Research, Geneva, Switzerland

3: Also at State Key Laboratory of Nuclear Physics and Technology, Peking University, Beijing, China

4: Also at Institut Pluridisciplinaire Hubert Curien, Université de Strasbourg, Université de Haute Alsace Mulhouse, CNRS/IN2P3, Strasbourg, France

5: Also at National Institute of Chemical Physics and Biophysics, Tallinn, Estonia

6: Also at Skobeltsyn Institute of Nuclear Physics, Lomonosov Moscow State University, Moscow, Russia

7: Also at Universidade Estadual de Campinas, Campinas, Brazil

8: Also at Centre National de la Recherche Scientifique (CNRS) - IN2P3, Paris, France

-
- 9: Also at Laboratoire Leprince-Ringuet, Ecole Polytechnique, IN2P3-CNRS, Palaiseau, France
 - 10: Also at Joint Institute for Nuclear Research, Dubna, Russia
 - 11: Also at Helwan University, Cairo, Egypt
 - 12: Now at Zewail City of Science and Technology, Zewail, Egypt
 - 13: Also at Beni-Suef University, Bani Sweif, Egypt
 - 14: Now at British University in Egypt, Cairo, Egypt
 - 15: Now at Ain Shams University, Cairo, Egypt
 - 16: Also at Université de Haute Alsace, Mulhouse, France
 - 17: Also at Tbilisi State University, Tbilisi, Georgia
 - 18: Also at University of Hamburg, Hamburg, Germany
 - 19: Also at Brandenburg University of Technology, Cottbus, Germany
 - 20: Also at Institute of Nuclear Research ATOMKI, Debrecen, Hungary
 - 21: Also at Eötvös Loránd University, Budapest, Hungary
 - 22: Also at University of Debrecen, Debrecen, Hungary
 - 23: Also at Wigner Research Centre for Physics, Budapest, Hungary
 - 24: Also at University of Visva-Bharati, Santiniketan, India
 - 25: Now at King Abdulaziz University, Jeddah, Saudi Arabia
 - 26: Also at University of Ruhuna, Matara, Sri Lanka
 - 27: Also at Isfahan University of Technology, Isfahan, Iran
 - 28: Also at University of Tehran, Department of Engineering Science, Tehran, Iran
 - 29: Also at Plasma Physics Research Center, Science and Research Branch, Islamic Azad University, Tehran, Iran
 - 30: Also at Università degli Studi di Siena, Siena, Italy
 - 31: Also at Purdue University, West Lafayette, USA
 - 32: Also at International Islamic University of Malaysia, Kuala Lumpur, Malaysia
 - 33: Also at Malaysian Nuclear Agency, MOSTI, Kajang, Malaysia
 - 34: Also at Consejo Nacional de Ciencia y Tecnología, Mexico city, Mexico
 - 35: Also at Warsaw University of Technology, Institute of Electronic Systems, Warsaw, Poland
 - 36: Also at Institute for Nuclear Research, Moscow, Russia
 - 37: Also at St. Petersburg State Polytechnical University, St. Petersburg, Russia
 - 38: Also at National Research Nuclear University 'Moscow Engineering Physics Institute' (MEPhI), Moscow, Russia
 - 39: Also at California Institute of Technology, Pasadena, USA
 - 40: Also at Faculty of Physics, University of Belgrade, Belgrade, Serbia
 - 41: Also at Facoltà Ingegneria, Università di Roma, Roma, Italy
 - 42: Also at National Technical University of Athens, Athens, Greece
 - 43: Also at Scuola Normale e Sezione dell'INFN, Pisa, Italy
 - 44: Also at University of Athens, Athens, Greece
 - 45: Also at Institute for Theoretical and Experimental Physics, Moscow, Russia
 - 46: Also at Albert Einstein Center for Fundamental Physics, Bern, Switzerland
 - 47: Also at Gaziosmanpasa University, Tokat, Turkey
 - 48: Also at Mersin University, Mersin, Turkey
 - 49: Also at Cag University, Mersin, Turkey
 - 50: Also at Piri Reis University, Istanbul, Turkey
 - 51: Also at Adiyaman University, Adiyaman, Turkey
 - 52: Also at Ozyegin University, Istanbul, Turkey
 - 53: Also at Izmir Institute of Technology, Izmir, Turkey
 - 54: Also at Mimar Sinan University, Istanbul, Istanbul, Turkey
 - 55: Also at Marmara University, Istanbul, Turkey

56: Also at Kafkas University, Kars, Turkey

57: Also at Yildiz Technical University, Istanbul, Turkey

58: Also at Hacettepe University, Ankara, Turkey

59: Also at Rutherford Appleton Laboratory, Didcot, United Kingdom

60: Also at School of Physics and Astronomy, University of Southampton, Southampton, United Kingdom

61: Also at Instituto de Astrofísica de Canarias, La Laguna, Spain

62: Also at Utah Valley University, Orem, USA

63: Also at University of Belgrade, Faculty of Physics and Vinca Institute of Nuclear Sciences, Belgrade, Serbia

64: Also at Argonne National Laboratory, Argonne, USA

65: Also at Erzincan University, Erzincan, Turkey

66: Also at Texas A&M University at Qatar, Doha, Qatar

67: Also at Kyungpook National University, Daegu, Korea